Acquired FGFR and FGF alterations confer resistance to estrogen receptor (ER) targeted therapy in ER+ metastatic breast cancer

Pingping Mao[1,2,3,4,£], Ofir Cohen[1,2,3,4,£], Kailey J. Kowalski[1,2,3,4], Justin G. Kusiel[1,2,3,4], Jorge E. Buendia-Buendia[1,2,3,4], Michael S. Cuoco[7], Pedro Exman[2], Seth A. Wander[1,2,3,4,5], Adrienne G. Waks[1,2,3,4,5], Utthara Nayar[1,2,3,4], Jon Chung[6], Samuel Freeman[4], Orit Rozenblatt-Rosen[7], Vincent A. Miller[6], Federica Piccioni[4], David E. Root[4], Aviv Regev[7,8], Eric P. Winer[2,3,5], Nancy U. Lin[2,3,5], Nikhil Wagle[1,2,3,4,5]

1. Center for Cancer Precision Medicine, Dana-Farber Cancer Institute, Boston, MA
2. Department of Medical Oncology, Dana-Farber Cancer Institute, Boston, MA
3. Harvard Medical School, Boston, MA
4. Broad Institute of MIT and Harvard, Cambridge, MA
5. Department of Medicine, Brigham and Women's Hospital, Boston, MA
6. Foundation Medicine, Inc. Cambridge, MA
7. Klarman Cell Observatory, Broad Institute of MIT and Harvard, Cambridge MA
8. Howard Hughes Medical Institute and Koch Institute of Integrative Cancer Research, Department of Biology, Massachusetts Institute of Technology, Cambridge, MA

Running title: FGFR/FGF alterations confer resistance to endocrine therapy

Key words: Drug resistance, endocrine therapy, ER+ breast cancer, FGF, FGFR

*Address correspondence to:
Nikhil Wagle, MD
Department of Medical Oncology
Dana-Farber Cancer Institute
450 Brookline Ave, Dana 820A
Boston, MA 02215
Phone: 617-632-6419
e-mail: nikhil_wagle@dfci.harvard.edu

£These authors contributed equally

Word count (excluding abstract, methods, references and figure legends): 6443
Total number of figures: 10

Competing Financial Interest Statement

S.A.W. is a consultant for Foundation Medicine and Eli Lilly, and a consultant and equity holder for InfiniteMD. J.C. is an employee/stockholder in Foundation Medicine, a wholly owned subsidiary of Roche. V.A.M. is an employee of Foundation Medicine/Roche, officer and board member of Revolution Medicines, and stockholder of Roche and Revolution Medicines. N.U.L is a consultant for Puma Biotechnology and Daichii, and

received research funding from Pfizer, Genentech, Novartis and Seattle Genetics. A.R. is a SAB member of ThermoFisher Scientific, Syros Pharmaceuticals, and Neogene Therapeutics, and a founder of and equity holder in Celsius Therapeutics. E.P.W. is a consultant for InfiniteMD, Genentech, and Eli Lilly. N.W. was previously a stockholder and consultant for Foundation Medicine; has been a consultant/advisor for Novartis and Eli Lilly; and has received sponsored research support from Novartis and Puma Biotechnology. None of these entities had any role in the conceptualization, design, data collection, analysis, decision to publish, or preparation of the manuscript

Abstract

Beyond acquired mutations in the estrogen receptor (ER), mechanisms of resistance to ER-directed therapies in ER+ breast cancer have not been clearly defined. We conducted a genome-scale functional screen spanning 10,135 genes to investigate genes whose overexpression confer resistance to selective estrogen receptor degraders. Pathway analysis of candidate resistance genes demonstrated that the FGFR, ERBB, insulin receptor, and MAPK pathways represented key modalities of resistance. In parallel, we performed whole exome sequencing in paired pre-treatment and post-resistance biopsies from 60 patients with ER+ metastatic breast cancer who had developed resistance to ER-targeted therapy. The FGFR pathway was altered via *FGFR1*, *FGFR2,* or *FGF3* amplifications or *FGFR2* mutations in 24 (40%) of the post-resistance biopsies. In 12 of the 24 post-resistance tumors exhibiting FGFR/FGF alterations, these alterations were not detected in the corresponding pre-treatment tumors, suggesting that they were acquired or enriched under the selective pressure of ER-directed therapy. *In vitro* experiments in ER+ breast cancer cells confirmed that FGFR/FGF alterations led to fulvestrant resistance as well as cross-resistance to the CDK4/6 inhibitor palbociclib. RNA sequencing of resistant cell lines treated with different drug combinations demonstrated that FGFR/FGF induced resistance through ER reprogramming and activation of the MAPK pathway. The resistance phenotypes were reversed by FGFR inhibitors, a MEK inhibitor, and/or a SHP2 inhibitor, suggesting potential treatment strategies. The detection of targetable, clonally acquired genetic alterations in the FGFR pathway in metastatic tumor biopsies highlights the value of serial tumor testing to dissect mechanisms of resistance in human breast cancer and its potential application in directing clinical management.

Introduction

Approximately 70% of breast cancers express the estrogen receptor (ER), and estrogen signaling drives breast cancer cell growth and progression [1]. Endocrine therapies are commonly used to treat ER+ breast cancer and work by reducing estrogen levels or targeting the estrogen receptor through functional inhibition or degradation. Although these endocrine therapies, including tamoxifen, aromatase inhibitors (AI), and the selective estrogen receptor degrader (SERD) fulvestrant have improved survival for ER+ breast cancer patients, within the metastatic setting resistance to endocrine therapies is nearly universal and remains a key challenge in reducing breast cancer morbidity and mortality [2].

Although various resistance mechanisms have been proposed for tamoxifen and aromatase inhibitor resistance, including loss or modification in ER expression (*ESR1* activating mutations and *ESR1* fusions) [3-7], and regulation of alternative signal transduction pathways (PI3K/AKT/mTOR and EGFR/ERBB2/MAPK) [8-10], mechanisms of resistance to SERDs remain understudied. Mechanisms of endocrine resistance identified in patients include acquired mutations in the estrogen receptor itself [4-7], acquired activating mutations in *ERBB2* (HER2) [11, 12], loss of function of *NF1* [13], and other alterations in MAPK pathway genes [14]. Additional mechanisms remain to be identified.

Gain-of-function screens have played a pivotal role in identification of resistance mechanisms to targeted therapies in various cancer types [15-17]. In breast cancer,

102 several functional screen studies identified *IGF1R*, *KRAS* and *ESR1* as mechanisms of
103 resistance to tamoxifen and/or estrogen deprivation [18-20]. However, genome-scale
104 functional screens for SERD resistance have not been reported.
105
106 We conducted a genome-scale gain-of-function screen in ER+ breast cancer cells
107 spanning 17,255 overexpressed lentiviral open reading frames (ORFs) to investigate
108 genes whose overexpression was sufficient to confer resistance to the SERDs fulvestrant
109 and GDC-0810 [21]. In parallel, we sought to identify endocrine resistance mechanisms
110 of clinical significance through genomic profiling of paired pre-treatment and post-
111 treatment tumor samples from 60 patients with ER+ metastatic breast cancer who
112 developed resistance to endocrine therapy.
113
114 The intersection of top candidate resistance mechanisms from both approaches converged
115 on the fibroblast growth factor receptor (FGFR) pathway. Here, we demonstrate that
116 acquired FGFR/FGF alterations identified in patients with resistant metastatic breast
117 cancer cause resistance to a variety of ER-directed therapies as well as to CDK4/6
118 inhibitors via MAPK pathway activation, and that this can be overcome by combination
119 therapy targeting ER, the FGFR pathway, and/or the MAPK pathway.
120
121 **Results**
122 ***A Genome-Scale Gain-of-Function Screen for Resistance to Selective Estrogen***
123 ***Receptor Degraders***

124 To identify the spectrum of genes whose overexpression confers resistance to SERDs *in*
125 *vitro*, we expressed 17,255 human open reading frames (ORFs), corresponding to 10,135
126 distinct human genes, in ER+ T47D breast cancer cells in the presence of fulvestrant or
127 GDC-0810. T47D cells were infected with the pooled lentiviral ORF library hORFeome
128 [22]. Fulvestrant, GDC-0810, or vehicle control (DMSO) was added following infection
129 and selection. ORF representation was assessed by sequencing after 21 days of drug
130 exposure. Genes that confer drug resistance will be enriched under drug selection,
131 indicated by a positive log fold change (LFC) for ORF representation before and after
132 DMSO/drug selection.
133
134 Using a Z score >3 as a criterion to identify resistance candidates, we identified 64 genes
135 (93 ORFs) that conferred resistance to fulvestrant and 57 genes (83 ORFs) that conferred
136 resistance to GDC-0810 (Fig.1A and Supplemental Table.1). 37 genes (55 ORFs)
137 conferred resistance to both drugs, a degree of overlap which was anticipated given the
138 mechanistic similarities between fulvestrant and GDC-0810. The LFC and corresponding
139 Z score for each ORF in fulvestrant and GDC-0810 treatment arms were highly
140 correlated, with a correlation coefficient of 0.77 (Fig.1A).
141
142 To confirm these results, we conducted a secondary screen using a smaller pooled library
143 consisting of 570 ORFs to validate candidates nominated by the primary screen. The
144 secondary screen was performed in both T47D and MCF7 cell lines with a similar screen
145 process as the primary screen. Top resistance genes found in the primary screen were
146 again enriched in the secondary screen, including *FGF* genes, *FOXR1*, *AKT* genes, *PIM*

147 genes and several *GPCR* genes (Supplemental Data Fig.S1). Many top ranked resistance
148 genes (*CSF1R, FGF3, FGF6, FOXR1* and *PIM2*) were shared between T47D and MCF7
149 cells (Supplemental Data Fig.S2). However, distinct resistance genes were also observed
150 in each cell line, suggesting some resistance mechanisms may be cell context-dependent.
151
152 Functional categories of candidate resistance genes include serine/threonine kinases
153 (*PIK3CA*, *AKT1/2/3*, *PIM1/2/3*), receptor tyrosine kinases (*EGFR*, *ERBB2, PDGFRB*),
154 growth factors (*FGF3/6/10/22*), cell cycle regulatory proteins (*CCND1*, *CCND2,*
155 *CCND3*, *CDK6*) and G-protein coupled receptors (*GPCR*) (Fig.1B). As further
156 validation, we overexpressed 13 ORFs belonging to these categories individually in
157 T47D cells and they conferred resistance to fulvestrant to various degrees (Fig.1C and
158 Supplemental Data Fig.S3A). Most of the 13 ORFs also conferred resistance to GDC-
159 0810 (Supplemental Data Fig.S3B).
160
161 Gene Set Enrichment Analysis (GSEA) of the candidate resistance genes demonstrated
162 enrichment in 4 functional pathways: FGFR signaling, ERBB signaling, insulin receptor
163 signaling, and the MAPK pathway (Fig.1D, Supplemental Data Fig.S4 and Supplemental
164 Table.2). Consistent with this, we recently demonstrated that acquired *ERBB2* activating
165 mutations activate the MAPK pathway and cause endocrine resistance in patients with
166 ER+ metastatic breast cancer [11]. Several recent studies have also shown that alterations
167 in MAPK pathway genes are enriched in endocrine-resistant tumors [13, 14]. We sought
168 to further examine the role of FGFR and FGF genes in resistance to SERDs in MBC.
169

170 ***Identification of acquired FGFR and FGF alterations in metastatic biopsies from***
171 ***patients with resistant ER+ MBC***
172 To examine the potential role of FGFR and FGF alterations in the development of
173 endocrine resistance clinically, we analyzed whole exome sequencing (WES) data from
174 paired pre-treatment and post-treatment metastatic tumor biopsies or cell free DNA from
175 60 patients with ER+ metastatic breast cancer who had received at least one endocrine
176 therapy (tamoxifen, AI, SERDs) for more than 120 days between the two biopsies [23].
177
178 Amongst the 60 post-treatment samples, we found *FGFR1* amplifications in 15% (9/60),
179 *FGFR2* amplifications in 5% (3/60), *FGFR2* activating mutations in 3.3% (2/60), and
180 *FGF3* amplifications in 28.3% (17/60) – for a total of 40% (24/60) of the cohort with at
181 least one alteration in one of these four genes (Fig.2A). Overall, the prevalence of
182 *FGFR1*, *FGFR2*, and *FGF3* alterations in the resistant metastatic setting seen here is
183 increased compared to what was observed in previously published cohorts of primary
184 ER+ breast cancer, such as The Cancer Genome Atlas (TCGA) [24] (Supplemental
185 Table.3). The incidence of *FGFR2* alterations (6.7%), in particular, is markedly increased
186 compared to primary treatment-naive breast cancer, in which the incidence is less than
187 2% in TCGA (Supplemental Table.3).
188
189 To determine if this enrichment of FGFR/FGF alterations in the metastatic setting was
190 due to acquisition/selection under the selective pressure of endocrine therapy, we
191 compared the WES from the paired pre-treatment and post-treatment samples for the 24
192 patients that exhibited FGFR/FGF alterations in their post-treatment samples. These 24

193 pairs of samples included 23 tumor biopsies and one cell-free DNA sample at the pre-
194 treatment timepoint, and 22 tumor biopsies and two cell-free DNA samples at the post-
195 treatment timepoint. We performed an evolutionary analysis to evaluate clonal structure
196 and dynamics, including changes in mutations and copy number. The evolutionary
197 inference and clonal dynamics of mutations was based on changes in the estimated
198 fraction of tumor cells harboring each genomic alteration (the cancer cell fraction, CCF)
199 as previously shown for acquired HER2 mutations [11]. The evolutionary inference of
200 copy number changes was based on measuring differences in copy number amplitudes
201 between pre-treatment and post-treatment samples, while accounting for differences in
202 cancer cell fraction ("purity") in the sample and correcting for differences in ploidy. The
203 resultant purity-corrected values provide an estimate of "copy number above ploidy"
204 (CNAP) (see Methods).
205
206 For this analysis, we define "acquired" alterations as alterations with higher
207 representation in the post-treatment sample as compared to the pre-treatment sample. For
208 single nucleotide variants (SNVs), this means that the mutation had a substantially higher
209 CCF in the post-treatment sample compared to the pre-treatment sample (including lack
210 of detection in the pre-treatment sample despite having sufficient power to detect the
211 mutation). For copy number changes, this means that there was a substantial increase in
212 the overall copy-number in the post-treatment sample. Although we use the term
213 "acquired", we recognize that when the mutation is not detected in the pre-treatment
214 sample, we cannot distinguish between pre-existing alteration that was selected for and
215 clonally enriched versus *de novo* alterations that developed during the treatment.

216

217 In 12 of the 24 patients with FGFR or FGF alterations (50%), the alterations were
218 acquired in the post-treatment sample as compared to the pre-treatment sample (Fig. 2A,
219 marked in red). Five out of nine *FGFR1* amplifications were acquired (55.6%), while all
220 four *FGFR2* alterations were acquired (100%), including one patient (Pt 0300350) with
221 acquisition of both an *FGFR2* mutation and amplification. *FGF3* amplifications were
222 acquired in 4 of 17 tumors (23.5%), including one case in which an *FGFR1* amplification
223 was co-acquired. The concurrent acquisition may suggest that the evolutionary selection
224 of both the ligand and receptor provided additional fitness in this tumor. Among the other
225 12 patients, the alterations in eight patients were shared in both pre-treatment and post-
226 treatment samples (Fig 2A, marked in black), and evolutionary status of alterations in the
227 remaining four patients was inconclusive (Fig 2A, marked in grey). The increase in copy
228 number (corrected for tumor purity and ploidy, Supplemental Table.4) from pre-treatment
229 to post-treatment for *FGFR1*, *FGFR2*, and the *FGF3* amplicon in all 12 patients is
230 depicted in Fig.2B.

231

232 Two of the acquired alterations found in these 12 patients were SNVs in the *FGFR2*
233 gene: M538I (chr10:123258070C>T, GRCh37, also denoted as M537I, depending on the
234 isoform) and N550K (chr10:123258034A>T, GRCh37, also denoted as N549K,
235 depending on the isoform). N550K is the most common FGFR2 mutation in breast cancer
236 while M538I was previously identified in lung cancer but has not yet been characterized
237 in breast cancer [25]. Figure 2C illustrates the change in the estimated fraction of tumor
238 cells harboring each genomic alteration (CCF) from the pre-treatment biopsy to the

239 resistant biopsy. In both patients, the *FGFR2* mutations were either not detected in the
240 primary tumor, despite sufficient power to detect mutations at this locus (N550K in Pt
241 0300350) or detected by a single read, inferred in a small fraction (CCF of 2%) of the
242 pre-treatment tumor (M538I in Pt 0300348). In both patients the activating *FGFR2*
243 mutations in the post-treatment biopsies were clonally acquired (CCF of 100%). Pt
244 0300350 was also found to have an acquired *FGFR2* amplification while Pt 0300348 was
245 found to have gained low-level amplification in *FGFR2* post treatment (Fig.2B).
246
247 Notably, the acquired alterations in *FGFR1*, *FGFR2*, and *FGF3* were largely mutually
248 exclusive with acquired *ESR1* mutations. *ESR1* mutations are the most common
249 mechanism described for acquired endocrine resistance [26]. Although the overall rate of
250 acquired *ESR1* mutation in this cohort is 22% (13/60), among the 12 cases of acquired
251 FGFR and FGF alterations, only one patient also has an acquired ESR1 mutation (Figure
252 2A). Similarly, only one of these 12 patients had acquired a HER2 mutation (which was
253 an alteration of unknown significance), suggesting that these are also mutually exclusive
254 mechanisms of resistance.
255
256 Although we highlight *FGF3* as the key gene in the amplicon (given the results of the
257 gain-of-function screen), *FGF3* resides in genomic proximity to *FGF4, FGF19* and
258 *CCND1* and these four genes are often co-amplified. Here, in 3 out of the 4 cases with
259 acquired *FGF3* amplification, *FGF3* copies were gained without co-acquisition of
260 *CCND1* amplification, suggesting that this acquisition can occur as an independent
261 genomic event. Similarly, 2 out of the 4 cases with acquired *FGF3* did not have co-

262 acquisition of *FGF19* amplification. In all 4 of the cases with *FGF3* amplification*, FGF4*
263 was also co-amplified. The relationship of acquisitions of *FGF3*, *FGF4, FGF19*, and
264 *CCND1* are depicted in Supplemental Data Fig.S5 and further details about these
265 amplicons are described in Supplemental Methods. Further exploration of the full
266 genomic contexts and other concurrent genetic alterations for the 12 patients with
267 acquired FGFR/FGF alterations are shown in Supplemental Data Fig.S6 and
268 Supplemental Table.5-6.
269
270 Figure 3 depicts clinical vignettes for six of the patients with acquired *FGFR1*, *FGFR2*,
271 and/or *FGF3* alterations in their post-treatment biopsies. All patients were treated with
272 ER-directed therapy before acquiring FGF or FGFR alterations, including tamoxifen (3
273 patients), AIs (6 patients), and fulvestrant (3 patients). Vignettes for the other six patients
274 with acquired *FGFR1*, *FGFR2*, and/or *FGF3* alterations in their post-treatment biopsies
275 are shown in Supplemental Data Fig.S7. Detailed clinicopathological features and
276 therapy details for all 12 patients are found in Supplemental Table.7.
277
278 In addition to these 12 patients in our cohort, we identified several additional patients
279 with acquired *FGFR1* and *FGFR2* activating mutations following the development of
280 resistance to endocrine therapy (Supplemental Data Fig.S8 and Supplemental Table.8).
281 FM patient 1 acquired a clonal *FGFR1* N546K mutation (a known activating mutation
282 paralogous to *FGFR2* N550K) following treatment with an AI. FM patient 2 acquired a
283 subclonal *FGFR2* N550K mutation after treatment with tamoxifen, AI and fulvestrant.

284 FM patient 3 acquired a subclonal *FGFR2* K660N mutation, another activating mutation
285 in the kinase domain [27], after treatment with tamoxifen.
286
287 In summary, we observed acquired alterations in *FGFR1*, *FGFR2*, or *FGF3* in 20%
288 (12/60) of patients with endocrine resistant ER+ MBC – comparable to the known
289 frequency of acquired mutations in *ESR1* – highlighting the important role of the FGFR
290 pathway in acquired resistance to ER-directed therapies.
291
292 ***Active FGFR signaling leads to resistance to SERDs through activation of the MAP***
293 ***kinase pathway***
294 To further investigate how FGFR/FGF genes may confer resistance to ER-directed
295 therapy, we treated T47D cells with FGF3, FGF6, FGF10 or FGF22 ligand. Each of these
296 ligands resulted in resistance to fulvestrant (Fig.4A). This effect was reversed by
297 PD173074, a pan-FGFR inhibitor (Fig.4A). The addition of these FGF ligands enhanced
298 phosphorylation of ERK and AKT, which was reversed by PD173074 (Fig.4B). The
299 effect of FGF ligands on downstream effectors was enhanced when FGFR1 was
300 simultaneously overexpressed in T47D, which has relatively low expression of FGFR1
301 [28] (Supplemental Data Fig.S9). FGF3, FGF6, FGF10 and FGF22 also reduced
302 fulvestrant sensitivity in MCF7 cells (Supplemental Data Fig. S10 A-B). Similar results
303 have been shown previously for FGF2, which was reported to activate MEK-ERK to
304 drive fulvestrant resistance in ER+ breast cancer cells [29].
305

306 We next overexpressed FGFR1, FGFR2, or GFP in T47D cells through lentiviral
307 transduction and examined the impact on susceptibility to SERDs. Overexpression of
308 FGFR1 or FGFR2 alone did not affect sensitivity to fulvestrant or GDC-0810. However,
309 with the addition of FGF2 ligand, both FGFR1 and FGFR2 rendered cells highly resistant
310 to the two SERDs (Fig. 4C and Supplemental Data Fig. S11). In comparison, FGF2
311 ligand alone reduced sensitivity to SERDs in control cells expressing GFP to a much
312 lesser extent than in the FGFR1 or FGFR2 expressing cells, suggesting the potent
313 resistance phenotype requires both FGF ligand and receptor. This requirement for the
314 presence of both FGF ligand and receptor for maximal resistance phenotype may also
315 explain why only FGFs but not FGFR1 or FGFR2 scored in the resistance screen (Fig.1
316 A-B). The resistance phenotype resulting from FGFR1 and FGFR2 overexpression was
317 completely reversed by the addition of PD173074 (Fig. 4C). Similar results were
318 obtained in MCF7 cells (Supplemental Data Fig.S12 A-B).
319
320 FGFR1 and FGFR2 overexpression (in the presence of FGF2 ligand) induced more
321 potent phosphorylation of AKT and ERK than the GFP control (Fig.4D). These results
322 are consistent with previous findings that FGFR1 activation led to MAPK activation and
323 fulvestrant resistance [28]. Activation of downstream effectors p-ERK and p-AKT by
324 FGFR1/2 overexpression was reversed to baseline levels with PD173074 (Fig. 4D and
325 Supplemental Data Fig. S12C). Examination of a larger number of kinases using kinase
326 antibody arrays demonstrated that AKT, ERK and RSK (downstream effector of ERK)
327 were the only kinases of those tested to exhibit increased phosphorylation following
328 FGFR1/2 overexpression and FGF2 stimulation (Supplemental Data Fig.S13).

329 Collectively, these findings suggest that FGFR1 and FGFR2 cause SERD resistance
330 through the activation of MAPK and/or PI3K/AKT pathways.
331
332 We examined the sensitivity of cells overexpressing FGFR1 or FGFR2 to several
333 inhibitors of downstream effectors: the MEK inhibitor trametinib, the AKT inhibitor
334 AZD5363, and the mTOR inhibitor everolimus. FGFR1 or FGFR2 overexpression in the
335 presence of FGF2 led to hypersensitivity to trametinib (Supplemental Data Fig.S14A),
336 but reduced sensitivity to AKT and mTOR inhibitors (Supplemental Data Fig.S14A).
337
338 We attempted to reverse FGFR-induced resistance to fulvestrant by inhibiting the MAPK
339 pathway. Treatment of FGFR1 overexpressing cells with trametinib partially resensitized
340 cells to fulvestrant, and treatment of FGFR2 overexpressing cells with trametinib fully
341 resensitized the cells to fulvestrant (Fig.4E-F). Treatment with the mTOR inhibitor
342 everolimus also partially reversed resistance conferred by FGFR1 or FGFR2
343 overexpression (Supplemental Data Fig.S14B). Colony formation assays produced
344 similar results (Supplemental Data Fig.S14C).
345
346 Together, these results suggest that the MAPK pathway is the primary downstream
347 effector of FGFR activation resulting in endocrine resistance. This is consistent with the
348 pathway analysis of resistance genes in our initial overexpression screen, which
349 demonstrated enrichment in MAPK pathway genes (Figure 1D), as well as our prior
350 findings of MAPK activation through acquired HER2 mutations in endocrine

351 resistance—adding further support to the idea that the MAPK pathway may be a common
352 node of endocrine resistance [11, 14].
353
354 ***FGFR activation confers cross-resistance to CDK4/6 inhibitors***
355 Since the combination of endocrine therapy and CDK4/6 inhibitors is now a standard of
356 care treatment for patients with ER+ metastatic breast cancer, we also examined the
357 effect of FGFR signaling on sensitivity to the combination of fulvestrant and the CDK4/6
358 inhibitor palbociclib. In T47D cells, FGFR1 and FGFR2 overexpression in the presence
359 of FGF2 also conferred resistance to combination treatment of fulvestrant and palbociclib
360 (Fig. 5A). The resistance phenotype was again abrogated by PD173074 (Fig. 5A).
361 Resistance to fulvestrant and palbociclib was also partially reversed by trametinib (Fig.
362 5B and Supplemental Data Fig. S14D), further providing the support for the role of
363 MAPK pathway activation in FGFR-mediated drug resistance. The reversal of resistance
364 by trametinib was accompanied by reduced ERK phosphorylation (Fig. 5C). Similar
365 results were achieved in MCF7 cells, although everolimus was more effective than
366 trametinib in reversing the resistance phenotype by FGFR1 or FGFR2 overexpression in
367 this cell line (Supplemental Data Fig.S15 and Fig.S16).
368
369 In the presence of fulvestrant and palbociclib, FGFR1 or FGFR2 overexpression was
370 accompanied by increased p-Rb and CCND1 levels, both of which were partially
371 reversed by trametinib (Fig.5C). CCND1 knockdown in cells overexpressing GFP,
372 FGFR1 or FGFR2 impaired cell proliferation similarly across all three cell lines without
373 affecting the IC50 of fulvestrant (Supplemental Data Fig.S17). This suggests that the

374 proliferation advantage provided by active FGFR signaling is partially dependent on
375 CCND1. This is consistent with prior results suggesting that CCND1 was involved in
376 FGF2-mediated drug resistance [29].
377
378 Clinical evidence also supports the finding that FGFR alterations can cause resistance to
379 CDK4/6 inhibitors. Following the acquisition of *FGFR2* N550K (along with *FGFR2*
380 amplification), Pt 0300350 did not respond to the combination of letrozole and
381 palbociclib (Fig.3), suggesting that *FGFR2* alterations may lead to intrinsic resistance to
382 the combination of endocrine therapy and CDK4/6 inhibitors. Another patient with an
383 *FGFR2* N550K mutation (FM Patient 2) also did not respond to the combination of
384 fulvestrant and palbociclib (Supplemental Data Fig.S8). Collectively, this suggests
385 targeting the FGFR pathway may also be a viable strategy to overcome FGFR/FGF-
386 mediated resistance to SERDs and CDK4/6 inhibitors.
387
388 ***FGFR2 mutations found in patients are activating with differential sensitivity to FGFR***
389 ***inhibitors***
390 We identified 3 acquired mutations in the kinase domain of FGFR2 in patients who
391 developed resistance to endocrine therapy. Two of these, FGFR2 N550K and K660N, are
392 known activating FGFR2 mutations that have been previously identified in breast cancer
393 [25, 27]. FGFR2 N550K is part of the molecular brake at the kinase hinge region, which
394 allows the receptor to adopt an active conformation more easily (Fig.6A). N550K is a
395 recurring hotspot mutation reported to confer resistance to several FGFR inhibitors
396 including PD173074 and dovitinib [30]. FGFR2 K660N is located in a conserved region

397 in the tyrosine kinase domain and has been confirmed to increase kinase activity [27, 30].
398 The third mutation, FGFR2 M538I, has not been previously reported in breast cancer.
399 Based on its location, M538I appears to stabilize the active kinase confirmation by
400 strengthening the hydrophobic spine of the FGFR2 kinase [30] (Fig.6A).
401
402 We expressed all three FGFR2 kinase domain mutants in T47D cells through lentiviral
403 transduction, as well as wildtype (WT) FGFR2 and GFP as negative controls. All three
404 mutants elicited higher kinase activity than WT FGFR2 constitutively, demonstrated by
405 levels of p-FRS2, a direct substrate for FGFR2 (Fig.6B). MAPK and AKT signaling were
406 also increased, as indicated by increased p-ERK and p-AKT levels, respectively (Fig.6B).
407 The addition of FGF2 ligand further enhanced downstream signaling for all FGFR2
408 mutants, and the enhanced signaling was blocked by PD173074 for FGFR2 M538I and
409 K660N, but not for N550K (Fig.6B).
410
411 FGFR2 mutants were also expressed under a tetracycline responsive promoter in T47D
412 cells grown in low doses of doxycycline to determine the functionality at lower
413 expression levels. At lower levels of expression, FGFR2 N550K still led to increased
414 levels of p-ERK and p-AKT, independent of FGF2 ligand stimulation. FGFR2 M538I
415 and K660N also resulted in higher p-ERK and p-AKT levels in the presence of FGF2 as
416 compared to FGFR2 WT (Fig.6C). Taken together, these results indicate that all three
417 FGFR2 mutations acquired in breast cancer patients are functionally active – FGFR2
418 N550K is constitutively active while FGFR2 M538I and K660N may be more ligand-
419 dependent at low levels of expression.

420

421 All 3 FGFR2 mutants led to modest resistance to fulvestrant (Fig.6D), which was
422 enhanced in the presence of FGF2 ligand. PD173074 resensitized cells overexpressing
423 FGFR2 M538I and FGFR2 K660N as well as WT FGFR2 to fulvestrant, but not cells
424 overexpressing FGFR2 N550K (Fig.6D). Consistent results were observed when cells
425 were treated with the combination of fulvestrant and palbociclib (Fig.6D). Similar results
426 were obtained in MCF7 cells (Supplemental Data Fig.S18).

427

428 ***Transcriptional changes induced by FGFR/FGF include ER reprograming and MAPK***
429 ***activation***

430 To examine transcriptional changes associated with FGFR pathway activation, we
431 performed RNA-Seq on ER+ T47D cells overexpressing FGFR1, FGFR2 (wildtype),
432 FGFR2 activating mutants (M538I, N550K, K660N), or FGF3, as well as on GFP and
433 parental lines as controls (Supplemental Table.9). We combined these profiles with
434 transcriptional profiles we previously generated [11] from of ER+ T47D cells
435 overexpressing wildtype and kinase-dead HER2, HER2 activating mutants (S653C,
436 L755S, V777L and L869R), and ESR1 Y537S, for a total of 15 genetic perturbations
437 examined.

438

439 Linear discriminant analysis of these profiles indicated that samples from cells
440 overexpressing FGFR1, FGFR2, FGFR2 activating mutants, FGF3, wildtype HER2, or
441 HER2 activating mutants are separated from controls (parental cells, GFP expressing, or
442 kinase-dead HER2 D845A) along the first LD component (LD1), as well as from a

443 separate group of cells overexpressing mutant ESR1 along the second LD component
444 (LD2), indicating a common RTK/growth factor-driven cell state that is distinct from the
445 mutant ER state (Fig. 7A). Along LD1, the cells overexpressing FGF3 have distinct
446 scores from those overexpressing FGFR (p.value = 2.12×10^{-10}, Welch's t-test), suggesting
447 that in our model system, FGF ligand overexpression is different from FGFR
448 overexpression (Fig. 7A). The overall signature strength of RTKs and growth-factor
449 signaling genes (defined in Supplemental Methods and shown in Supplemental Table.10)
450 were highly correlated with scores on LD1 (Spearman's rho= 0.926), suggesting that LD1
451 broadly represents RTK and growth-factor pathway activation.
452
453 Using differential expression analysis to compare activating constructs with controls, we
454 defined transcriptional signatures FGFR1/2, FGF3, and HER2-MUT. The FGFR1/2
455 signature was generated by comparing FGFR1, FGFR2, FGFR2 M538I, FGFR2 N550K,
456 and FGFR2 K660N overexpression (all with FGF2 ligand) to parental and GFP (with and
457 without FGF2 ligand). The FGF3 signature was generated by comparing FGF3
458 overexpression (without FGF2 ligand) to parental and GFP (with and without FGF2
459 ligand). The HER2-MUT signature was generated by comparing the HER2 activating
460 mutants (HER2 S653C, L755S, V777L and L869R) with GFP controls.
461
462 Comparison of the top 200 highly expressed genes in each of the FGFR1/2, FGF3, and
463 HER2-MUT signatures (Supplemental Table.11) highlights the high degree of similarity
464 between these groups, with 32 genes common to the FGFR1/2 and FGF3 signatures
465 (Odds-ratio=39.63 p.value=4.7×10^{-37}, two-sided Fisher's exact test), 84 genes common to

466 the FGFR1/2 and HER2-MUT signatures (Odds-ratio=219.4, p.value=1.025×10^{-140}, two-
467 sided Fisher's exact test), and 18 upregulated genes common to all 3 groups (Fig 7B).
468
469 We next defined an FGF/R-ACT transcriptional state based on 377 genes that are
470 upregulated in FGF3 and FGFR1/2 cell lines compared with controls (Fig. 7C and
471 Supplemental Table.10). Gene Set Enrichment Analysis [31] of the FGF/R-ACT state vs.
472 5,150 previously characterized gene sets (Supplemental Table.12) demonstrated that the
473 shared FGF/R-ACT state is enriched for upregulation of RTK/growth factor receptors
474 signaling, RAS/MAPK signaling, and growth factor–induced ER target genes (Fig. 7D-
475 F), similar to what we have previously shown for HER2 activating mutants [11]. This is
476 consistent with a model in which FGFR/FGF activation leads to ER reprogramming via
477 MAPK pathway activation, potentially shifting the transcriptional spectrum from genes
478 activated by transcription factor AF2 to those activated by AF1. Of note, the genes
479 associated with mTOR signaling were variably upregulated and downregulated in
480 FGF/R-ACT state (Fig. 7G), suggesting only moderate mTOR activation as compared to
481 the robust MAPK activation signal observed. Similar transcriptional signatures were seen
482 when the FGF/R-ACT signature was characterized under fulvestrant treatment,
483 demonstrating that the FGF/R-ACT state is present even when ER signaling is inhibited,
484 consistent with the phenotype of fulvestrant resistance (Supplemental Table.11-12).
485
486 ***Activating FGFR2 mutations can be targeted with irreversible FGFR inhibitors***
487 FGFR2 M538I and N550K have been shown to confer resistance to multi-kinase inhibitor
488 dovitinib in BaF3 cells, and N550K is also resistant to PD173074 (Fig.6 B and D)[30].

489 Because of the differential responses of these FGFR2 mutants to PD173074, we tested
490 the ability of additional FGFR inhibitors to resensitize cells expressing these mutants to
491 fulvestrant. FIIN-2 and FIIN-3 are two irreversible covalent pan-FGFR inhibitors that
492 target a cysteine conserved in FGFR1-4 and have exquisite selectivity for some FGFR2
493 mutations including M538I and K659N [32]. In addition, AZD4547 is a selective FGFR
494 inhibitor that was previously shown to inhibit FGFR2 N550K [33].
495
496 Both FIIN-2 and FIIN-3 were more effective in inhibiting the downstream signaling (p-
497 FRS2, p-ERK and p-AKT) induced by FGFR2 N550K as compared to PD173074 and
498 AZD4547 (Fig.8A). Furthermore, FIIN compounds reduced the level of downstream
499 effectors back to baseline levels, with FIIN-3 being more potent than FIIN-2
500 (Supplemental Data Fig.S19). T47D cells stably overexpressing FGFR2 mutant were
501 exquisitely sensitive to FIIN-2 and FIIN-3 as compared to cells expressing GFP or
502 FGFR2 WT (Supplemental Fig.S20). The resistance to fulvestrant induced by both WT
503 FGFR2 and all mutant FGFR2 was completely blocked by FIIN-2 (1 μM) and FIIN-3
504 (100 nM), but not by PD173074 (1 μM) and AZD4547 (1 μM) (Fig.8B). While resistance
505 to WT FGFR1/2 and FGFR2 M538I and FGFR2 K660N can be reversed by multiple
506 FGFR inhibitors, for some mutants like FGFR2 N550K, only the irreversible pan-FGFR
507 inhibitors successfully resensitized cells to fulvestrant, highlighting the fact that specific
508 resistance mutations might require different strategies to overcome or preempt endocrine
509 resistance.
510

511 Next, we evaluated the effect of ten different drug combinations on the transcriptional
512 signatures in FGFR/FGF expressing cell lines and control cells profiled by RNA-seq. The
513 activated RAS/MAPK signature, ER signaling driven by growth factors signature, and
514 FGF/R-ACT signature present in cells overexpressing FGFR/FGF constructs persisted
515 under treatment with fulvestrant, palbociclib, or their combination (Fig. 9). Treatment
516 with FIIN-3, alone or in combination with fulvestrant and/or palbociclib largely reversed
517 the activation of all three signatures (Supplemental Table.13). For example, all
518 FGFR/FGF constructs showed suppression of FGF/R-ACT signature by FIIN-3 treatment
519 (FIIN-3 vs. DMSO, median effect size = -5.42, Cohen's D test with Hedges correction;
520 median p.value = 7.858×10^{-6}, Welch's t-test), albeit with less suppression observed for
521 FGF3 (effect size = -1.86, p.value = 0.00028) and FGFR2 N550K (effect size = -3.74,
522 p.value = 6.722×10^{-5}) constructs (Fig. 9; Supplemental Table.13). Effective suppression
523 of all three signatures was also achieved by trametinib plus fulvestrant, with or without
524 palbociclib (Fig. 9; Supplemental Table 13),
525
526 ***Targeting MAPK pathway via SHP2 inhibition can overcome FGFR-induced***
527 ***endocrine resistance***
528 Data from the gain-of-function ORF screen, the transcriptomic analysis, and our
529 individual *in vitro* experiments together suggest that MAPK pathway may represents a
530 common node for drug resistance in ER+ metastatic breast cancer. FGFR2 mutants, in
531 particular, rendered cells more sensitive to trametinib than did GFP or WT FGFR2
532 (Fig.10A), further supporting the finding that FGFR signaling requires the MAPK
533 pathway in this context. Src homology phosphotyrosyl phosphatase 2 (SHP2) is protein

534 downstream of RTKs that is required for RAS activation. Several recent studies have
535 demonstrated that co-targeting SHP2 prevented adaptive resistance to MEK inhibition in
536 multiple RAS-driven cancer models[34-36]. Consistent with this, cell lines expressing
537 FGFR2 mutants were hypersensitive to the SHP2 inhibitor SHP099 (Fig.10B). We next
538 examined the ability of combinations of SHP099, trametinib, fulvestrant, and/or
539 palbociclib to overcome resistance in FGFR-expressing cell lines. Similar to trametinib,
540 SHP099 as a single agent partially rescued resistance to fulvestrant and/or palbociclib
541 conferred by FGFR1, and completely rescued resistance conferred by FGFR2. Cells
542 expressing the FGFR2 constructs (wildtype or activating mutations) were particularly
543 sensitive to the treatment regimen of trametinib and SHP099 in addition to fulvestrant
544 and palbociclib (Fig.10C-D), in comparison with minimal inhibitory effect of MEK and
545 SHP2 inhibition in GFP control cells. The cell viability phenotype was accompanied with
546 consistent changes in p-ERK levels; SHP099 alone partially reduced ERK
547 phosphorylation and the combination of SHP099 and trametinib completely abrogated p-
548 ERK levels (Supplemental Fig.S21). These results suggest that targeting MEK and SHP2
549 may serve as an even more effective strategy to overcome multiple forms of FGFR
550 pathway mediated resistance to endocrine therapy and CDK4/6 inhibitors in MBC, as
551 well as, potentially, other RTK-induced mechanisms of resistance.
552

553 **Discussion**

554 In this study, we used a genome-scale gain-of-function screen to identify potential
555 mechanisms of resistance to selective estrogen receptor degraders. We nominated several
556 different candidate resistance genes and pathways, particularly genes in the ERBB

557 pathway, FGFR pathway, insulin receptor signaling and the MAPK pathway. Consistent
558 with this finding, genomic profiling of paired pre-treatment and post-treatment tumor
559 samples from 60 patients with ER+ metastatic breast cancer who developed resistance to
560 endocrine therapy identified acquired alterations in *FGFR1*, *FGFR2*, and *FGF3* in 20%
561 of patients. Experimental studies confirmed that these alterations confer resistance to
562 endocrine therapy as well as CDK4/6 inhibitors, through activation of MAPK pathway,
563 and demonstrated that this resistance can be reversed by FGFR inhibitors, MEK and
564 SHP2 inhibitors. Taken together, our results suggest that activating FGFR pathway
565 alterations are a distinct mechanism of acquired resistance to multiple forms of ER-
566 directed therapy in MBC that can be overcome by FGFR and/or MAPK pathway
567 inhibitors.
568
569 Our findings are consistent with two recently published results. Formisano, Arteaga, and
570 colleagues identified *FGFR1* amplification as a mechanism of resistance to CDK4/6
571 inhibitors [37]. In another study, Drago et al. demonstrated that FGFR1 amplification
572 confers resistance to ER, PI3K and CDK4/6 inhibitors while retaining TORC sensitivity
573 [38]. Our results also extend our understanding of endocrine resistance with multiple
574 novel findings. Experimentally, this includes functional screen data for SERD resistance
575 that includes over 10,000 genes that implicate multiple novel pathways and genes in
576 endocrine resistance. It also includes evidence showing that FGFR1
577 overexpression, FGFR2 overexpression, FGF3 overexpression, and the specific three
578 FGFR2 mutants found in patients *all* result in resistance to endocrine therapy and/or
579 CDK4/6 inhibitors that can be overcome by specific targeted therapies. Clinically, the

580 WES analysis of 60 pairs of pre-treatment and post-resistance tumor biopsies identified
581 multiple alterations in the FGFR pathway in post endocrine therapy tumor biopsies,
582 including FGF3 amplifications as well as FGFR1 and FGFR2 alterations. Most
583 significantly, we present here a rigorous demonstration that 50% of cases these
584 FGFR/FGF pathway alterations are *acquired* after resistance to therapy.
585
586 Our genome-scale screen provided a comprehensive view into the resistance mechanisms
587 to SERDs. Similar resistance genes were nominated for fulvestrant and GDC-0810,
588 thereby confirming the two drugs have similar mechanism of action. Of note, two ESR1
589 ORFs conferred resistance specifically to GDC-0810 but not fulvestrant, possibly due to
590 GDC-0810 having a less potent effect on ER degradation than fulvestrant [21, 39].
591 Among the resistance mechanisms shared by fulvestrant and GDC-0810, many are
592 frequently altered in ER+ MBC, such as *CCNDs/CDK6*, *KRAS/MAPK*, *EGFR/ERBB2*
593 and *PIK3CA/AKTs/PIMs*, and agents targeting those alterations are under clinical
594 development to be combined with endocrine therapy [14, 40]. We also identified
595 potential resistance mechanisms that are not characterized to the same extent, such as G
596 protein-coupled receptors, Wnt pathway (*FZD10, RSPO1, RSPO3*) and Src family
597 kinases (*YES1, FYN, FGR*), providing clues as to the potential crosstalk between these
598 pathways and ER signaling [41-43] and suggesting that breast cancer patients harboring
599 functional alterations in these pathways may develop resistance to SERDs. Notably, some
600 of the resistance genes were also nominated in gain-of-function screens designed to
601 identify resistance mechanisms for MAPK pathway inhibitors in melanoma (*AXL, CRK,*
602 *CRKL, FGR, GPCR* genes) [15] and PI3K inhibitors in ER+ breast cancer (*AKT1, AKT2,*

603 *CRKL, FGF3, FGF10, PIM* genes) [17]. This may reveal multi-drug resistance
604 mechanisms and thus guide clinical drug combinations to overcome resistance. We have
605 provided the full genome-scale screen data as a resource to the community of researchers
606 interested in resistance to ER-directed therapies as well as the biology of estrogen
607 receptor dependencies in ER+ breast cancer.
608
609 Our ultimate goal is to identify resistance mechanisms that are clinically relevant and can
610 be therapeutically targeted. By comparing paired pre-treatment and post-treatment
611 tumors, our evolutionary analyses identified acquired *FGFR1* and *FGFR2*, and *FGF3*
612 alterations in 12 out of 60 post-treatment samples, further highlighting a potential role for
613 the FGFR pathway in driving drug resistance and disease progression.
614 Most notably, all four alterations in FGFR2 in our cohort were found to be acquired after
615 the development of resistance to endocrine therapy. Our overall findings are consistent
616 with other recent studies which noted some patients with acquired *FGFR1* and *FGFR2*
617 alterations following treatment of endocrine therapy [37, 38, 44, 45], and provides a
618 mechanistic explanation for these acquisitions.
619
620 This analysis was enabled by a novel method we developed to compare the magnitude of
621 amplification in matched pre- and post-treatment samples while considering key
622 confounders to allow for more reliable assignment of copy gain or loss. Since matched
623 tumor samples of the same patient are highly variable in the cancer cell fraction (purity)
624 and often variable in ploidy (with genome duplication taking place in the metastatic
625 setting), we computed the purity-corrected copy number above ploidy and set a relatively

626 stringent threshold of changes in CNAP to define acquired amplification (see Methods),
627 as cancer clones bearing amplifications with high focality and magnitude in FGFR/FGF
628 genes are more likely to induce dependency on FGFR pathway and result in endocrine
629 resistance.
630
631 Our genomic analysis has some limitations and caveats. The observed alterations may not
632 exclusively result from endocrine therapy as some patients received other therapies
633 between the two collected biopsies. Moreover, tumors with FGFR/FGF alterations also
634 harbor alterations in other cancer genes, which may contribute to drug resistance as well
635 (Supplemental Data Fig.S6 and Supplemental Table.5). Despite these caveats, with the
636 evidence from unbiased screens, genomic evidence in relevant patient samples, and
637 confirmatory experimental models, the FGFR pathway clearly emerges as a clinically
638 important resistance mechanism for SERDs and CDK4/6 inhibitors.
639
640 Strategies to target the FGFR pathway in breast cancer patients with FGFR alterations are
641 currently being assessed in clinical trials. FGFR inhibitors currently under clinical
642 development in breast cancer include non-selective tyrosine kinase inhibitors (dovitinib
643 and lucitanib), FGFR1-3 selective inhibitors (AZD4547 and BGJ398), and others,
644 although clinical trials have achieved mixed results to date [46-51]. The combination of
645 FGFR inhibitors and endocrine therapy is also being clinically investigated. For example,
646 the combination of dovitinib and fulvestrant showed promising clinical activity [46]. As
647 FGFR pathway activation also results in resistance to CDK4/6 inhibitors, a triple
648 combination with the addition of CDK4/6 inhibitors may also be considered. One

649 challenge for the use of FGFR inhibitors is to identify reliable biomarkers. Our results
650 suggest focal and high level amplifications, clonal activating mutations or high
651 expression levels of FGFR and FGF genes, particularly in the metastatic setting, may be
652 used to guide the clinical use of FGFR inhibitors. Activating alterations in *FGFR2*, which
653 are rare in primary treatment naïve breast cancer but appear to be clonally acquired in a
654 subset of patients with resistant ER+ MBC, may be a particularly good biomarker for the
655 development of FGFR inhibitors.
656
657 Our work also highlights that the effective clinical use of FGFR inhibitors needs to
658 consider the variable drug sensitivity of different FGFR2 mutations, which were acquired
659 in some patients following endocrine therapy. The two irreversible pan-FGFR kinase
660 inhibitors, FIIN-2 and FIIN-3, had superior efficacy in targeting all FGFR2 mutants
661 including N550K when compared to other FGFR inhibitors, although *in vivo* efficacy,
662 off-target effects and toxicity of FIIN compounds still warrant further investigation.
663
664 Alterations in FGFR1 and FGFR2 activated the MAPK pathway, and MEK inhibition
665 was able to overcome the resistance conferred by FGFR pathway to some degree. We
666 previously demonstrated acquired ERBB2 mutations resulted in a reprogrammed ER
667 signature and an elevated MAPK transcriptional signature [11]. In this study, the
668 transcriptional analysis results suggest that MAPK activation resulting from FGFR/FGF
669 overexpression is more pronounced than mTOR activation, which had a mixed signature.
670 This is consistent with our experimental findings, which demonstrated that MAPK
671 inhibition is particularly effective in cells expressing FGFR2 activating alterations. Other

672 MAPK genes were also found to be enriched in the gain-of-function screen. Furthermore,
673 increased frequency of alterations in MAPK pathway genes have been found in tumors
674 post hormonal therapy, including *EGFR, ERBB2* and *NF1* [14]. The fact that multiple
675 mechanisms of resistance to ER-directed therapies and/or CDK4/6 inhibitors activate the
676 MAPK pathway suggests that this may be an important node of resistance in ER+ MBC.
677 Thus, combining endocrine therapy and CDK4/6 inhibitors with agents that target MAPK
678 pathway, such as MEK inhibitors and/or SHP2 inhibitors [52, 53], may be a unifying
679 strategy to overcome or prevent resistance resulting from multiple genetic aberrations
680 that lead to resistance in ER+ MBC.
681
682 In summary, the integration of a functional genomic screen and genomic analysis of pre-
683 and post-treatment biopsies revealed the FGFR pathway as an important resistance
684 mechanism for endocrine therapy and CDK4/6 inhibitors in ER+ breast cancer. With the
685 increasing use of SERDs and CDK4/6 inhibitors in the clinic, we anticipate that the
686 prevalence of FGFR/FGF alterations might increase in the future. Targeting the FGFR
687 pathway with FGFR inhibitors or agents that target downstream MAPK signaling may
688 improve clinical outcomes in patients with aberrations in FGFR/FGF genes. Furthermore,
689 our study highlights the need to sequence metastatic biopsy or blood biopsies at the time
690 of resistance to identify patients with these alterations who may benefit from targeting the
691 FGFR pathway.
692

693 **Methods**

694 ***Cell culture***

695 293T, T47D and MCF7 cells were purchased from American Type Culture Collection

696 (ATCC) and were cultured as described in the Supplemental Methods.

697

698 ***Genome-Scale Gain-of-Function Screen***

699 The pooled lentiviral ORF library hORFeome [22] consists of 17,255 barcoded human

700 open reading frames (ORFs), corresponding to 10,135 distinct human genes with at least

701 99% nucleotide and protein match. These ORFs were cloned into pLX317 vector and

702 pooled together for transfection into 293T cells to make pooled lentivirus (with 2nd

703 generation packaging plasmids). In 6-well plates, pooled lentivirus was infected in cells

704 to achieve ~50% infection rate and ensure ~1000 infected cells per ORF for 17255.

705 Media was supplemented with 4 μg/mL polybrene (Thermo Fisher Scientific #

706 TR1003G) to boost transfection efficiency. After infection, cells were pooled and

707 selected with 1.5 μg/mL puromycin for 5 days. Upon completion of selection, cells were

708 plated for three different drug conditions: DMSO, 100 nM fulvestrant, 1 μM GDC-0810.

709 There were three replicates for each condition screened. A subset of cells was saved for

710 sequencing as early time point (ETP) samples to confirm ORF representation. The dose

711 for each drug was chosen for the two drugs to achieve potent anti-proliferation effect that

712 could be rescued with ESR1 mutant Y537N and Y537S. Infected cells were passaged

713 upon confluency and maintained in DMSO or drugs for 21 days to allow sufficient time

714 for cells carrying resistance to be enriched from the population. At the end of the time

715 course, cells were harvested for isolating genomic DNA as late time point samples (LTP).

716 All genomic DNA samples were amplified with PCR primers flanking the ORF region
717 and sequenced. The ORF representation at the final harvesting (LTP) is compared to the
718 representation of ORFs in cells collected before drug addition (ETP). Cells carrying
719 ORFs that are driving resistance will grow and gradually enrich the population and
720 therefore, will be over-represented in the sequencing data for the final passage compared
721 to the early time point. An ORF with significant enrichment (a Z score >3) is defined as a
722 resistance candidate gene. A secondary validation screen was performed as described in
723 the Supplemental Methods.
724
725 ***Patients and Tumor Samples***
726 Prior to any study procedures, all patients provided written informed consent for research
727 biopsies and whole exome sequencing of tumor and normal DNA, as approved by the
728 Dana-Farber/Harvard Cancer Center Institutional Review Board (DF/HCC Protocol 05-
729 246). Metastatic core biopsies were obtained from patients and samples were
730 immediately snap frozen in OCT and stored in -80°C. Archival FFPE blocks of primary
731 tumor samples were also obtained. A blood sample was obtained during the course of
732 treatment, and whole blood was stored at -80°C until DNA extraction from peripheral
733 blood mononuclear cells (for germline DNA) was performed. In a few instances, cell free
734 DNA was obtained from plasma for circulating tumor DNA analysis, as previously
735 described[54].
736
737

738 ***Whole Exome (WES) analysis***

739 DNA was extracted from primary tumors, metastatic tumors, plasma, and peripheral
740 blood mononuclear cells (for germline DNA) from all patients and whole exome
741 sequencing was performed, as detailed in the Supplemental Methods. Sequencing data
742 were analyzed using tools to identify somatic point mutations and small
743 insertions/deletions (indels), and copy number changes using established algorithms (see
744 Supplemental Methods).

745

746 To better measure segment-specific copy-number, we subtracted the genome ploidy for
747 each sample to compute copy number above ploidy (CNAP). CNAP of at least 3 are
748 considered as amplifications (AMP), CNAP below 3 are considered low amplification
749 and ignored in our analysis). CNAP of at least 6 are considered high amplifications
750 (HighAMP), and CNAP of at least 9 and fewer than 100 genes [55] is considered very
751 high focal amplification (FocalAMP).

752

753 The evolutionary classification of amplifications accounts for the magnitude of the
754 observed copy-number difference between the pre-treatment and the post-treatment
755 samples. If the difference between the CNAP of the post-treatment and the CNAP of the
756 pre-treatment is smaller than 50%, the amplification is defined as “Shared”. If the CNAP
757 of the post-treatment is larger than the CNAP by more than 50% and the lower pre-
758 treatment CNAP is not at “FocalAMP” level, the evolutionary classification is
759 “Acquired”. If CNAP of the post-treatment is smaller by at least 50%, comparing to the
760 pre-treatment sample and the lower post-treatment CNAP is not at “FocalAMP” level, the

761 evolutionary classification is “Loss”. Otherwise, the evolutionary classification of
762 amplifications is defined as “Indeterminate”.
763
764 ***RNA-seq characterization of genomically perturbed cells under various drug***
765 ***conditions***
766 We performed RNA-Seq on T47D cells perturbed to overexpress FGFR pathway
767 activation including FGFR1, FGFR2 (WT, K660N, M538I and N550K), and FGF3, as
768 well as GFP and parental as a control, as described above. Cells were plated in 96-well
769 plates, and then treated with DMSO, fulvestrant (100 nM), palbociclib (1 μM), FIIN-3
770 (100 nM), and trametinib (500 nM) as single agent and in combinations for 24 hours.
771 FGFR1/2 cell lines were treated with or without FGF2 (10 ng/mL) in various conditions.
772 RNA was extracted from cells and sequencing libraries prepared as described in
773 Supplementary Methods. For each specific construct and treatment combination we
774 performed at least 6 replicates, for a total of 672 RNA-Seq profiles.
775
776 ***Generation of plasmids and engineered cells***
777 T47D or MCF7 cells were infected with lentivirus to derive stable cell lines
778 overexpressing wildtype (WT) or mutant ORFs. All WT ORFs were obtained from the
779 Broad Institute. Mutant ORFs (FGFR2 M538I, N550K and K660N) were made using
780 QuickChange II site-directed mutagenesis kit (Agilent Technologies #200523). Most
781 stable cells lines express ORFs in pLX317 vector and were selected with puromycin (Life
782 Technologies #A1113803). Stable cell lines expressing CCND1 and PIM1 in pLX304
783 vector were selected with blasticidin (Life Technologies #A1113903).

784

785 For inducible cell lines, WT or Mutant FGFR2 IIIb ORFs were cloned into pInducer20
786 Tetracycline-inducible lentiviral vector (Addgene #44012) using gateway cloning
787 technology (Invitrogen #11791019). Lentivirus was then generated and infected to
788 establish Tet-inducible cells lines cultured in 10% Tet-system approved FBS (Clontech
789 #631106) and 500 µg/mL G418 (Life Technologies #10131035). Doxycycline (Clontech
790 #631311) was used to induce ORF expression.

791

792 ***Kill curves and CellTiter-Glo viability assay***

793 Cells were plated in 96-well tissue culture ViewPlate (Perkin Elmer # 6005181) on Day 1
794 and treated with drug on Day 2. Media with or without drugs was refreshed on Day 5. On
795 Day 8, cells were equilibrated to room temperature, media was removed, and cells were
796 lysed in a mixture of 50 µL media and 50 µL CellTiter-Glo 2.0 reagent (Promega #
797 G9243) per well. Plates were then incubated on an orbital shaker for 2 mins. Following
798 another 10 mins of incubation at room temperature to stabilize signal, luminescence was
799 recorded to measure cell viability on Infinite M200 Pro microplate reader (Tecan).

800

801 ***Colony formation assay***

802 2,000-30,000 cells were plated in 6-well plates on Day 1 and treated on Day 2. Media
803 was refreshed every 3-4 days until crystal violet staining. On the day of staining, cells
804 were fixed with ice-cold 100% methanol for 10 minutes and then incubated with 0.5%
805 crystal violet solution (Sigma Aldrich #C6158) in 25% methanol at room temperature for
806 10 minutes.

807

808 ***Western blotting***

809 Western blotting was performed as described in supplemental methods.

810

811 ***Statistical analysis***

812 Statistical analyses related to drug response curve were performed with two-tailed student
813 t-test in Graphpad Prism. Fisher's exact test was used to calculate odds ratio and q-value
814 for volcano plots in the RNA sequencing analysis. Cohen's D test with Hedges correction
815 and Welch's t-test were used to estimate the effect size and significance for signature
816 strength of gene sets.

817

818 **Data availability**

819 Tumor and germline whole exome sequencing data generated and analyzed for this study
820 will be deposited in the access-controlled public repository dbGAP
821 (https://www.ncbi.nlm.nih.gov/gap). Additional data generated in this study including
822 tumor exome analysis and RNA-seq data are available within the paper and in the
823 supplementary information files.

824

825 **Acknowledgements**

826 We thank Qaren Quartey, Christian Kapstad and Gabriela Johnson for technical
827 assistance; Karla Helvie, Laura Dellostritto, Lori Marini, Nelly Oliver, Shreevidya
828 Periyasamy, Colin Mackichan, Max Lloyd, and Mahmoud Charif for assistance with
829 patient sample collection and annotation; and Flora Luo, Tinghu Zhang and Nathanael

Gray for providing reagents. We thank Jorge Gómez Tejeda Zañudo for helpful discussions and comments on the manuscript. We are grateful to all the patients who volunteered for our tumor biopsy protocol and generously provided the tissue analyzed in this study.

Grant support

This work was supported by the Department of Defense W81XWH-13-1-0032 (N.W.), AACR Landon Foundation 13-60-27-WAGL (N.W.), NCI Breast Cancer SPORE at DF/HCC #P50CA168504 (N.W., N.U.L and E.P.W), Susan G. Komen CCR15333343 (N.W.), The V Foundation (N.W.), The Breast Cancer Alliance (N.W.), The Cancer Couch Foundation (N.W.), Twisted Pink (N.W.), Hope Scarves (N.W.), Breast Cancer Research Foundation (N.U.L. and E.P.W.), ACT NOW (to Dana-Farber Cancer Institute Breast Oncology Program), Fashion Footwear Association of New York (to Dana-Farber Cancer Institute Breast Oncology Program), Friends of Dana-Farber Cancer Institute (to N.U.L.), Stand Up to Cancer (N.W.), National Science Foundation (N.W.), SU2C-TVF Convergence Scholarship (P.M.), and The American Association for Cancer Research Basic Science Fellowship (P.M.).

Author contributions

P.M., O.C. and N.W. conceived and designed the study; P.M. K.K. and J.K. performed experiments; O.C. and J.B. performed the computational analyses with input from S.F.; P.E., S.A.W., A.G.W., and N.W. performed clinical data abstraction and annotation; P.M. and M.S.C performed the RNA sequencing experiments; O.R. helped with the execution

853 of the RNA-Seq; A.R. helped with the RNA-Seq data analysis; U.N. performed the prior
854 HER2 mutant RNA sequencing experiments; J.C., V.M., and M.C. provided the clinical
855 and genomic data for the 3 patients in the Foundation Medicine cohort; F.P and D.R.
856 helped with the design and execution of the ORF screen; E.P.W., N.U.L., and N.W.
857 oversaw patient enrollment and sample collection on the metastatic biopsy protocol;
858 P.M., O.C. and N.W. wrote the manuscript with input from all authors; N.W. supervised
859 the study.

860 **References**

861

862 1. Chen WY, Colditz GA: **Risk factors and hormone-receptor status:**
863 **epidemiology, risk-prediction models and treatment implications for breast**
864 **cancer**. *Nature clinical practice Oncology* 2007, **4**(7):415-423.

865 2. Osborne CK, Schiff R: **Mechanisms of endocrine resistance in breast cancer**.
866 *Annual review of medicine* 2011, **62**:233-247.

867 3. Lei JT, Gou X, Ellis MJ: **ESR1 fusions drive endocrine therapy resistance and**
868 **metastasis in breast cancer**. *Molecular & cellular oncology* 2018,
869 **5**(6):e1526005.

870 4. Robinson DR, Wu YM, Vats P, Su F, Lonigro RJ, Cao X, Kalyana-Sundaram S,
871 Wang R, Ning Y, Hodges L *et al*: **Activating ESR1 mutations in hormone-**
872 **resistant metastatic breast cancer**. *Nature genetics* 2013, **45**(12):1446-1451.

873 5. Toy W, Shen Y, Won H, Green B, Sakr RA, Will M, Li Z, Gala K, Fanning S,
874 King TA *et al*: **ESR1 ligand-binding domain mutations in hormone-resistant**
875 **breast cancer**. *Nature genetics* 2013, **45**(12):1439-1445.

876 6. Merenbakh-Lamin K, Ben-Baruch N, Yeheskel A, Dvir A, Soussan-Gutman L,
877 Jeselsohn R, Yelensky R, Brown M, Miller VA, Sarid D *et al*: **D538G mutation**
878 **in estrogen receptor-alpha: A novel mechanism for acquired endocrine**
879 **resistance in breast cancer**. *Cancer Res* 2013, **73**(23):6856-6864.

880 7. Jeselsohn R, Yelensky R, Buchwalter G, Frampton G, Meric-Bernstam F,
881 Gonzalez-Angulo AM, Ferrer-Lozano J, Perez-Fidalgo JA, Cristofanilli M,
882 Gomez H *et al*: **Emergence of constitutively active estrogen receptor-alpha**
883 **mutations in pretreated advanced estrogen receptor-positive breast cancer**.
884 *Clin Cancer Res* 2014, **20**(7):1757-1767.

885 8. Garcia-Becerra R, Santos N, Diaz L, Camacho J: **Mechanisms of resistance to**
886 **endocrine therapy in breast cancer: focus on signaling pathways, miRNAs**
887 **and genetically based resistance**. *International journal of molecular sciences*
888 2012, **14**(1):108-145.

889 9. Miller TW, Perez-Torres M, Narasanna A, Guix M, Stal O, Perez-Tenorio G,
890 Gonzalez-Angulo AM, Hennessy BT, Mills GB, Kennedy JP *et al*: **Loss of**
891 **Phosphatase and Tensin homologue deleted on chromosome 10 engages**
892 **ErbB3 and insulin-like growth factor-I receptor signaling to promote**
893 **antiestrogen resistance in breast cancer**. *Cancer Res* 2009, **69**(10):4192-4201.

894 10. Massarweh S, Osborne CK, Jiang S, Wakeling AE, Rimawi M, Mohsin SK,
895 Hilsenbeck S, Schiff R: **Mechanisms of tumor regression and resistance to**
896 **estrogen deprivation and fulvestrant in a model of estrogen receptor-positive,**
897 **HER-2/neu-positive breast cancer**. *Cancer Res* 2006, **66**(16):8266-8273.

898 11. Nayar U, Cohen O, Kapstad C, Cuoco MS, Waks AG, Wander SA, Painter C,
899 Freeman S, Persky NS, Marini L *et al*: **Acquired HER2 mutations in ER(+)**
900 **metastatic breast cancer confer resistance to estrogen receptor-directed**
901 **therapies**. *Nature genetics* 2018.

902 12. Croessmann S, Formisano L, Kinch LN, Gonzalez-Ericsson PI, Sudhan DR, Nagy
903 RJ, Mathew A, Bernicker EH, Cristofanilli M, He J *et al*: **Combined Blockade of**
904 **Activating ERBB2 Mutations and ER Results in Synthetic Lethality of**
905 **ER+/HER2 Mutant Breast Cancer**. *Clin Cancer Res* 2019, **25**(1):277-289.

906 13. Sokol ES, Feng YX, Jin DX, Basudan A, Lee AV, Atkinson JM, Chen J, Stephens
907 PJ, Frampton GM, Gupta PB *et al*: **Loss of function of NF1 is a mechanism of**
908 **acquired resistance to endocrine therapy in lobular breast cancer**. *Ann Oncol*
909 2019, **30**(1):115-123.

910 14. Razavi P, Chang MT, Xu G, Bandlamudi C, Ross DS, Vasan N, Cai Y, Bielski
911 CM, Donoghue MTA, Jonsson P *et al*: **The Genomic Landscape of Endocrine-**
912 **Resistant Advanced Breast Cancers**. *Cancer cell* 2018, **34**(3):427-438 e426.

913 15. Johannessen CM, Johnson LA, Piccioni F, Townes A, Frederick DT, Donahue
914 MK, Narayan R, Flaherty KT, Wargo JA, Root DE *et al*: **A melanocyte lineage**
915 **program confers resistance to MAP kinase pathway inhibition**. *Nature* 2013,
916 **504**(7478):138-142.

917 16. Wilson FH, Johannessen CM, Piccioni F, Tamayo P, Kim JW, Van Allen EM,
918 Corsello SM, Capelletti M, Calles A, Butaney M *et al*: **A functional landscape of**
919 **resistance to ALK inhibition in lung cancer**. *Cancer cell* 2015, **27**(3):397-408.

920 17. Le X, Antony R, Razavi P, Treacy DJ, Luo F, Ghandi M, Castel P, Scaltriti M,
921 Baselga J, Garraway LA: **Systematic Functional Characterization of**
922 **Resistance to PI3K Inhibition in Breast Cancer**. *Cancer discovery* 2016,
923 **6**(10):1134-1147.

924 18. Gonzalez-Malerva L, Park J, Zou L, Hu Y, Moradpour Z, Pearlberg J, Sawyer J,
925 Stevens H, Harlow E, LaBaer J: **High-throughput ectopic expression screen for**
926 **tamoxifen resistance identifies an atypical kinase that blocks autophagy**.
927 *Proceedings of the National Academy of Sciences of the United States of America*
928 2011, **108**(5):2058-2063.

929 19. Fox EM, Miller TW, Balko JM, Kuba MG, Sanchez V, Smith RA, Liu S,
930 Gonzalez-Angulo AM, Mills GB, Ye F *et al*: **A kinome-wide screen identifies**

931 **the insulin/IGF-I receptor pathway as a mechanism of escape from hormone**
932 **dependence in breast cancer**. *Cancer research* 2011, **71**(21):6773-6784.

933 20. Mendes-Pereira AM, Sims D, Dexter T, Fenwick K, Assiotis I, Kozarewa I,
934 Mitsopoulos C, Hakas J, Zvelebil M, Lord CJ *et al*: **Genome-wide functional**
935 **screen identifies a compendium of genes affecting sensitivity to tamoxifen**.
936 *Proceedings of the National Academy of Sciences of the United States of America*
937 2012, **109**(8):2730-2735.

938 21. Joseph JD, Darimont B, Zhou W, Arrazate A, Young A, Ingalla E, Walter K,
939 Blake RA, Nonomiya J, Guan Z *et al*: **The selective estrogen receptor**
940 **downregulator GDC-0810 is efficacious in diverse models of ER+ breast**
941 **cancer**. *eLife* 2016, **5**.

942 22. Yang X, Boehm JS, Yang X, Salehi-Ashtiani K, Hao T, Shen Y, Lubonja R,
943 Thomas SR, Alkan O, Bhimdi T *et al*: **A public genome-scale lentiviral**
944 **expression library of human ORFs**. *Nature methods* 2011, **8**(8):659-661.

945 23. Cohen O, Kim D, Oh C, Waks A, Oliver N, Helvie K, Marini L, Rotem A, Lloyd
946 M, Stover D *et al*: **Abstract S1-01: Whole exome and transcriptome**
947 **sequencing of resistant ER+ metastatic breast cancer**. *Cancer Research* 2017,
948 **77**(4 Supplement):S1-01.

949 24. Cancer Genome Atlas N: **Comprehensive molecular portraits of human breast**
950 **tumours**. *Nature* 2012, **490**(7418):61-70.

951 25. Gallo LH, Nelson KN, Meyer AN, Donoghue DJ: **Functions of Fibroblast**
952 **Growth Factor Receptors in cancer defined by novel translocations and**
953 **mutations**. *Cytokine Growth Factor Rev* 2015, **26**(4):425-449.

954 26. Jeselsohn R, Buchwalter G, De Angelis C, Brown M, Schiff R: **ESR1 mutations-**
955 **a mechanism for acquired endocrine resistance in breast cancer**. *Nat Rev Clin*
956 *Oncol* 2015, **12**(10):573-583.

957 27. Reintjes N, Li Y, Becker A, Rohmann E, Schmutzler R, Wollnik B: **Activating**
958 **somatic FGFR2 mutations in breast cancer**. *PloS one* 2013, **8**(3):e60264.

959 28. Turner N, Pearson A, Sharpe R, Lambros M, Geyer F, Lopez-Garcia MA,
960 Natrajan R, Marchio C, Iorns E, Mackay A *et al*: **FGFR1 amplification drives**
961 **endocrine therapy resistance and is a therapeutic target in breast cancer**.
962 *Cancer Res* 2010, **70**(5):2085-2094.

963 29. Shee K, Yang W, Hinds JW, Hampsch RA, Varn FS, Traphagen NA, Patel K,
964 Cheng C, Jenkins NP, Kettenbach AN *et al*: **Therapeutically targeting tumor**
965 **microenvironment-mediated drug resistance in estrogen receptor-positive**
966 **breast cancer**. *The Journal of experimental medicine* 2018, **215**(3):895-910.

967 30. Byron SA, Chen H, Wortmann A, Loch D, Gartside MG, Dehkhoda F, Blais SP,
968 Neubert TA, Mohammadi M, Pollock PM: **The N550K/H mutations in FGFR2**
969 **confer differential resistance to PD173074, dovitinib, and ponatinib ATP-**
970 **competitive inhibitors**. *Neoplasia* 2013, **15**(8):975-988.

971 31. Sergushichev AA: **An algorithm for fast preranked gene set enrichment**
972 **analysis using cumulative statistic calculation**. *bioRxiv* 2016:060012.

973 32. Tan L, Wang J, Tanizaki J, Huang Z, Aref AR, Rusan M, Zhu SJ, Zhang Y, Ercan
974 D, Liao RG *et al*: **Development of covalent inhibitors that can overcome**
975 **resistance to first-generation FGFR kinase inhibitors**. *Proc Natl Acad Sci U S*
976 *A* 2014, **111**(45):E4869-4877.

977 33. Yu M, Bardia A, Aceto N, Bersani F, Madden MW, Donaldson MC, Desai R,
978 Zhu H, Comaills V, Zheng Z *et al*: **Cancer therapy. Ex vivo culture of**
979 **circulating breast tumor cells for individualized testing of drug susceptibility**.
980 *Science* 2014, **345**(6193):216-220.

981 34. Ahmed TA, Adamopoulos C, Karoulia Z, Wu X, Sachidanandam R, Aaronson
982 SA, Poulikakos PI: **SHP2 Drives Adaptive Resistance to ERK Signaling**
983 **Inhibition in Molecularly Defined Subsets of ERK-Dependent Tumors**. *Cell*
984 *reports* 2019, **26**(1):65-78 e65.

985 35. Fedele C, Ran H, Diskin B, Wei W, Jen J, Geer MJ, Araki K, Ozerdem U,
986 Simeone DM, Miller G *et al*: **SHP2 Inhibition Prevents Adaptive Resistance to**
987 **MEK Inhibitors in Multiple Cancer Models**. *Cancer discovery* 2018,
988 **8**(10):1237-1249.

989 36. Ruess DA, Heynen GJ, Ciecielski KJ, Ai J, Berninger A, Kabacaoglu D, Gorgulu
990 K, Dantes Z, Wormann SM, Diakopoulos KN *et al*: **Mutant KRAS-driven**
991 **cancers depend on PTPN11/SHP2 phosphatase**. *Nature medicine* 2018,
992 **24**(7):954-960.

993 37. Formisano L, Lu Y, Servetto A, Hanker AB, Jansen VM, Bauer JA, Sudhan DR,
994 Guerrero-Zotano AL, Croessmann S, Guo Y *et al*: **Aberrant FGFR signaling**
995 **mediates resistance to CDK4/6 inhibitors in ER+ breast cancer**. *Nature*
996 *communications* 2019, **10**(1):1373.

997 38. Drago JZ, Formisano L, Juric D, Niemierko A, Servetto A, Wander SA, Spring
998 LM, Vidula N, Younger J, Peppercorn J *et al*: **FGFR1 gene amplification**
999 **mediates endocrine resistance but retains TORC sensitivity in metastatic**
1000 **hormone receptor positive (HR+) breast cancer**. *Clin Cancer Res* 2019.

1001 39. Guan J, Zhou W, Hafner M, Blake RA, Chalouni C, Chen IP, De Bruyn T,
1002 Giltnane JM, Hartman SJ, Heidersbach A *et al*: **Therapeutic Ligands**

1003 **Antagonize Estrogen Receptor Function by Impairing Its Mobility**. *Cell* 2019,
1004 **178**(4):949-963 e918.

1005 40. AlFakeeh A, Brezden-Masley C: **Overcoming endocrine resistance in hormone**
1006 **receptor-positive breast cancer**. *Curr Oncol* 2018, **25**(Suppl 1):S18-S27.

1007 41. Loh YN, Hedditch EL, Baker LA, Jary E, Ward RL, Ford CE: **The Wnt**
1008 **signalling pathway is upregulated in an in vitro model of acquired tamoxifen**
1009 **resistant breast cancer**. *BMC Cancer* 2013, **13**:174.

1010 42. Won HS, Lee KM, Oh JE, Nam EM, Lee KE: **Inhibition of beta-Catenin to**
1011 **Overcome Endocrine Resistance in Tamoxifen-Resistant Breast Cancer Cell**
1012 **Line**. *PloS one* 2016, **11**(5):e0155983.

1013 43. Vallabhaneni S, Nair BC, Cortez V, Challa R, Chakravarty D, Tekmal RR,
1014 Vadlamudi RK: **Significance of ER-Src axis in hormonal therapy resistance**.
1015 *Breast cancer research and treatment* 2011, **130**(2):377-385.

1016 44. Yates LR, Knappskog S, Wedge D, Farmery JHR, Gonzalez S, Martincorena I,
1017 Alexandrov LB, Van Loo P, Haugland HK, Lilleng PK *et al*: **Genomic Evolution**
1018 **of Breast Cancer Metastasis and Relapse**. *Cancer cell* 2017, **32**(2):169-184
1019 e167.

1020 45. O'Leary B, Cutts RJ, Liu Y, Hrebien S, Huang X, Fenwick K, Andre F, Loibl S,
1021 Loi S, Garcia-Murillas I *et al*: **The Genetic Landscape and Clonal Evolution of**
1022 **Breast Cancer Resistance to Palbociclib plus Fulvestrant in the PALOMA-3**
1023 **Trial**. *Cancer discovery* 2018, **8**(11):1390-1403.

1024 46. Musolino A, Campone M, Neven P, Denduluri N, Barrios CH, Cortes J,
1025 Blackwell K, Soliman H, Kahan Z, Bonnefoi H *et al*: **Phase II, randomized,**
1026 **placebo-controlled study of dovitinib in combination with fulvestrant in**
1027 **postmenopausal patients with HR(+), HER2(-) breast cancer that had**
1028 **progressed during or after prior endocrine therapy**. *Breast Cancer Res* 2017,
1029 **19**(1):18.

1030 47. Andre F, Bachelot T, Campone M, Dalenc F, Perez-Garcia JM, Hurvitz SA,
1031 Turner N, Rugo H, Smith JW, Deudon S *et al*: **Targeting FGFR with dovitinib**
1032 **(TKI258): preclinical and clinical data in breast cancer**. *Clin Cancer Res*
1033 2013, **19**(13):3693-3702.

1034 48. Smyth EC, Turner NC, Pearson A, Peckitt C, Chau I, Watkins DJ, Starling N, Rao
1035 S, Gillbanks A, Kilgour E *et al*: **Phase II study of AZD4547 in FGFR amplified**
1036 **tumours: Gastroesophageal cancer (GC) cohort pharmacodynamic and**
1037 **biomarker results**. *Journal of Clinical Oncology* 2016, **34**(4_suppl):154-154.

1038 49. Babina IS, Turner NC: **Advances and challenges in targeting FGFR signalling**
1039 **in cancer**. *Nat Rev Cancer* 2017, **17**(5):318-332.

1040 50. Chae YK, Ranganath K, Hammerman PS, Vaklavas C, Mohindra N, Kalyan A,
1041 Matsangou M, Costa R, Carneiro B, Villaflor VM *et al*: **Inhibition of the**
1042 **fibroblast growth factor receptor (FGFR) pathway: the current landscape**
1043 **and barriers to clinical application**. *Oncotarget* 2017, **8**(9):16052-16074.

1044 51. Nogova L, Sequist LV, Perez Garcia JM, Andre F, Delord JP, Hidalgo M,
1045 Schellens JH, Cassier PA, Camidge DR, Schuler M *et al*: **Evaluation of BGJ398,**
1046 **a Fibroblast Growth Factor Receptor 1-3 Kinase Inhibitor, in Patients With**
1047 **Advanced Solid Tumors Harboring Genetic Alterations in Fibroblast**
1048 **Growth Factor Receptors: Results of a Global Phase I, Dose-Escalation and**
1049 **Dose-Expansion Study**. *Journal of clinical oncology : official journal of the*
1050 *American Society of Clinical Oncology* 2017, **35**(2):157-165.

1051 52. Matalkah F, Martin E, Zhao H, Agazie YM: **SHP2 acts both upstream and**
1052 **downstream of multiple receptor tyrosine kinases to promote basal-like and**
1053 **triple-negative breast cancer**. *Breast Cancer Res* 2016, **18**(1):2.

1054 53. Chen YN, LaMarche MJ, Chan HM, Fekkes P, Garcia-Fortanet J, Acker MG,
1055 Antonakos B, Chen CH, Chen Z, Cooke VG *et al*: **Allosteric inhibition of SHP2**
1056 **phosphatase inhibits cancers driven by receptor tyrosine kinases**. *Nature*
1057 2016, **535**(7610):148-152.

1058 54. Adalsteinsson VA, Ha G, Freeman SS, Choudhury AD, Stover DG, Parsons HA,
1059 Gydush G, Reed SC, Rotem D, Rhoades J *et al*: **Scalable whole-exome**
1060 **sequencing of cell-free DNA reveals high concordance with metastatic**
1061 **tumors**. *Nature communications* 2017, **8**(1):1324.

1062 55. Ulz P, Belic J, Graf R, Auer M, Lafer I, Fischereder K, Webersinke G, Pummer
1063 K, Augustin H, Pichler M *et al*: **Whole-genome plasma sequencing reveals**
1064 **focal amplifications as a driving force in metastatic prostate cancer**. *Nature*
1065 *communications* 2016, **7**:12008.
1066

Figure 1

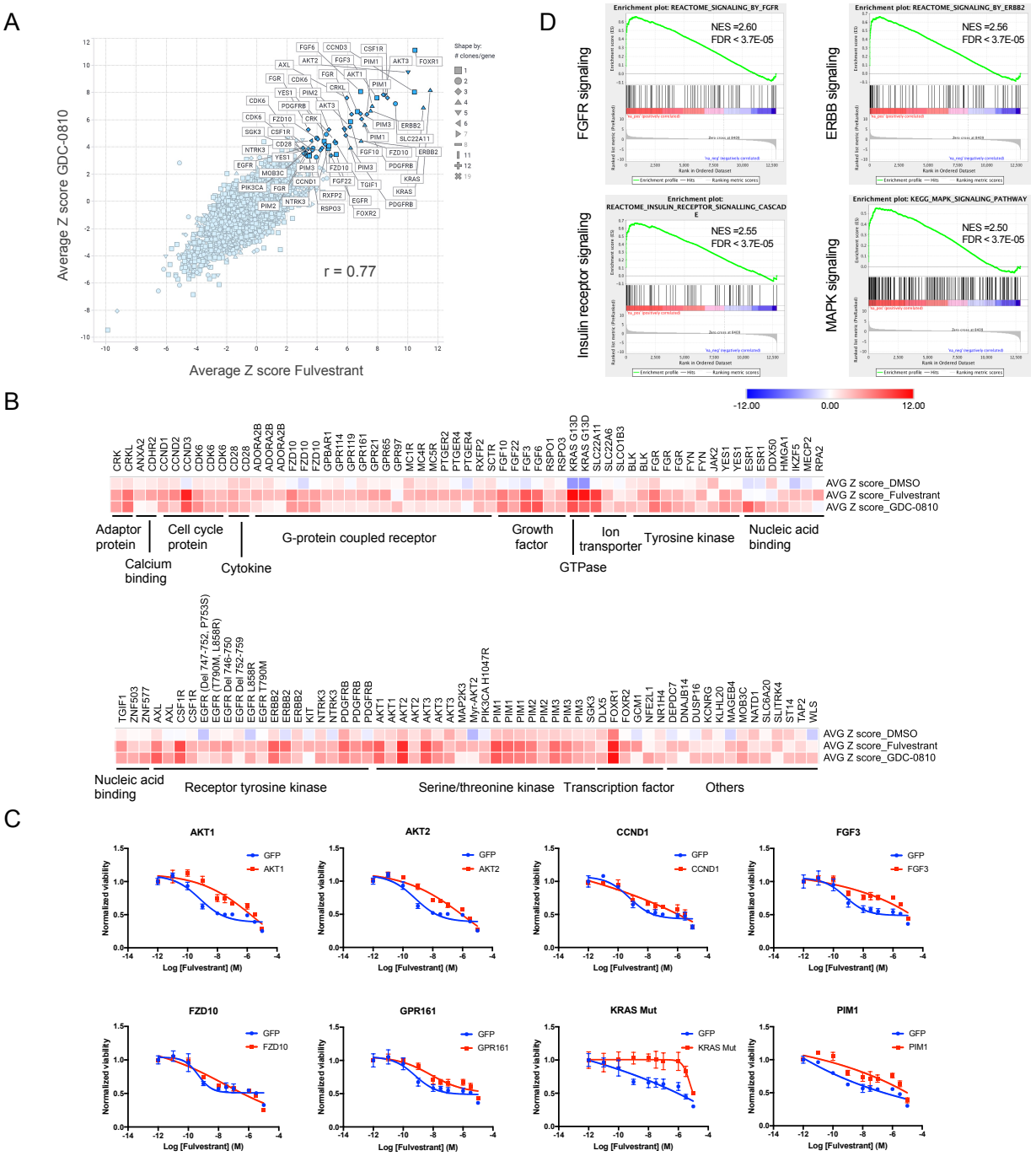

Figure 1. A genome-scale gain-of-function screen identified resistance genes to fulvestrant and GDC-0810. 17,255 human open reading frames (ORFs), corresponding to 10,135 distinct genes, were expressed in ER+ T47D breast cancer cells in the presence of fulvestrant or GDC-0810. Fulvestrant, GDC-0810, or vehicle control (DMSO) was added following infection and selection. ORF representation was assessed by sequencing after 21 days of drug exposure. Genes that confer drug resistance will be enriched under drug selection, indicated by a positive log fold change (LFC) for ORF representation before and after DMSO/drug selection. A, The average Z score for LFC of each ORF was plotted for both the fulvestrant (X-axis) and GDC-0810 (Y-axis) arms. The average Z score was calculated from three replicates in each condition. The ORFs with a Z score > 3 in both drug arms are highlighted and labeled with gene ID. The shape of each data point represents the total number of ORFs for that gene in the library. B, Heatmap of top ORF hits with a Z score > 3 in fulvestrant or GDC-0810 arm. The Z score in the DMSO arm is also presented. ORF hits are grouped by their molecular function according to Uniprot annotation. Information on the complete list of ORFs can be found in Supplemental Table.1. C, Individual ORFs were overexpressed in T47D cells and validated to confer resistance to fulvestrant by drug response curves. *KRAS* G12D ORF was used for overexpression in T47D cells while other selected ORFs are wildtype. Cell viability was measured by CellTiter-Glo and all the data points were normalized to growth under DMSO condition. Results shown are ± SD and representative of three independent experiments. D, Gene set enrichment analysis was performed for the gene list ranked by LFC in the fulvestrant arm. For genes with multiple ORFs, the ORF with highest LFC was selected. 1000 permutations were performed for the analysis. NES, normalized enrichment score. The full list of nominated pathways is shown in Supplemental Table.2.

Figure 2

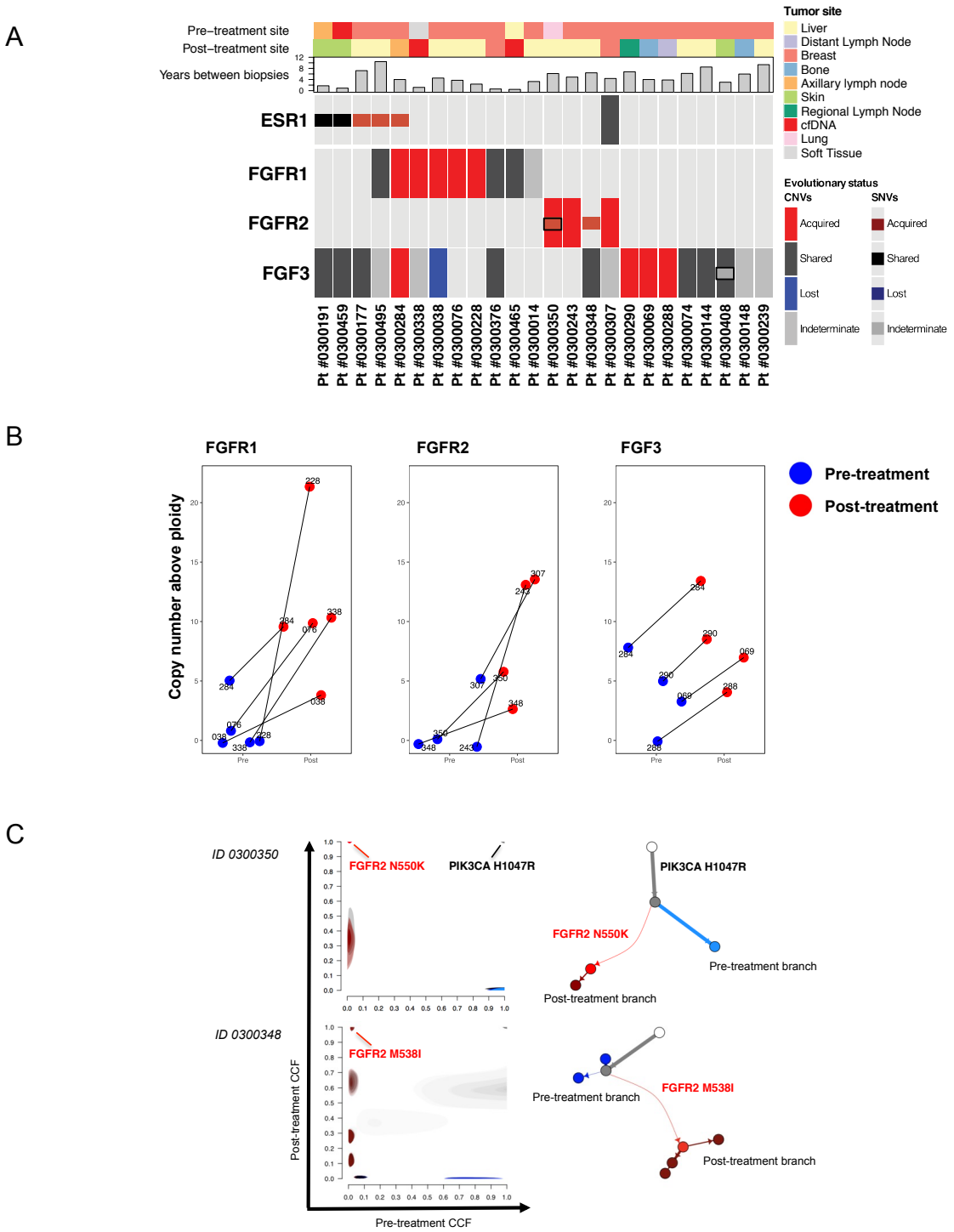

Figure 2. Identification of acquired FGFR and FGF alterations in metastatic biopsies from patients with resistant ER+ MBC. A, Evolutionary status of *ESR1*, *FGFR1*, *FGFR2*, and *FGF3* alterations is presented by comparing the pre-treatment and post-treatment mutational status for each patient (red = acquired, blue = lost, black = shared, grey = indeterminate). Clinical and pathology tracks depict the site of biopsy for both matched samples, and the duration between the pre-treatment and post-treatment biopsies. B, Copy number alterations for *FGFR1*, *FGFR2* and *FGF3* in pre- and post-treatment tumor samples are shown with copy number above ploidy (CNAP) depicted to illustrate the magnitude of the acquired amplification in each case. To better measure segment-specific copy number, we subtracted the genome ploidy for each sample to compute CNAP. The purity and ploidy for tumor samples are shown in Supplemental Table.4. C, Clonal evolution analysis showing the overall clonal structure and acquisition for FGFR2 mutations observed in two patients. In the pre-treatment biopsies, *FGFR2* M538I (*ID 0300348*) and *FGFR2* N550K (*ID 0300350*) were with cancer cell fraction (CCF) of 2% (single read) and 0% (unobserved), respectively, while being observed as clonal mutations in the post-treatment sample with a CCF of 1. The phylogenetic relationships among clones are reconstructed for each patient starting from the normal cell (white circle) connected to the ancestral cancer cells (grey trunk). The phylogenetic divergence to the pre-treatment clones (and subclones) is depicted with blue edges, and phylogenetic divergence to the metastatic clones (and subclones) is in red. Selected mutations in cancer genes are marked on the corresponding branches of the cancer phylogeny.

Figure 3

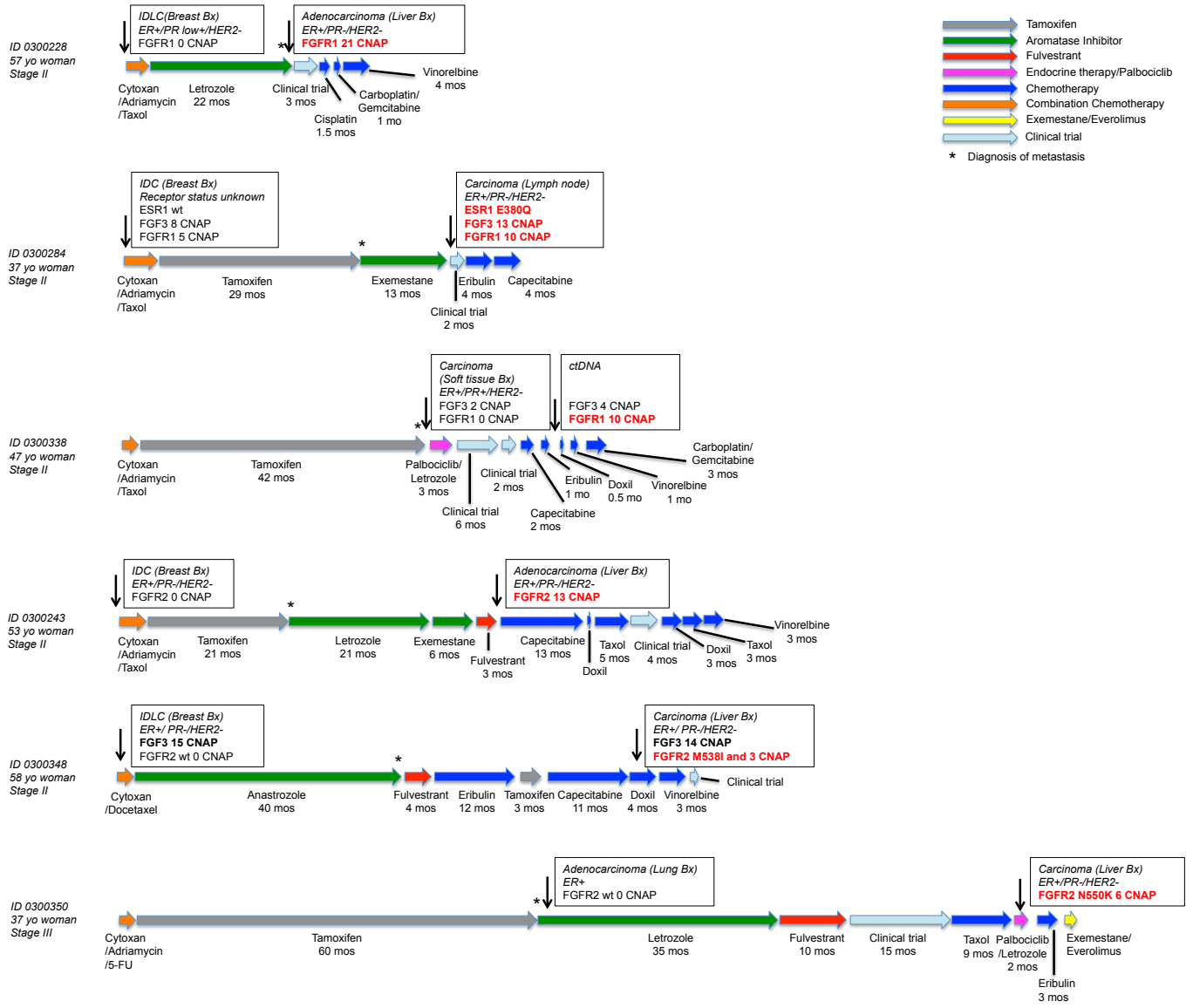

Figure 3. Clinical vignettes of patients who acquired FGFR/FGF alterations following endocrine therapy. The clinical vignettes for selected patients with acquired alterations in *FGFR1*, *FGFR2*, and/or *FGF3* illustrate detailed information on age and stage of disease at diagnosis, therapies patients received, duration of response to each therapy, and time of biopsies collected during the clinical course. For each biopsy, available information on biopsy type, tissue site, receptor status and selected genomic alterations detected by whole exome sequencing is shown. In each case, the asterisk indicates the time that metastatic disease was diagnosed. The complete clinicopathologic information for each patient is provided in Supplemental Table.7. IDC: invasive ductal carcinoma, IDLC: invasive ductal-lobular carcinoma; CNAP: copy number above ploidy; yo: years old; Bx: biopsy; PR: progesterone receptor; wt: wildtype.

Figure 4

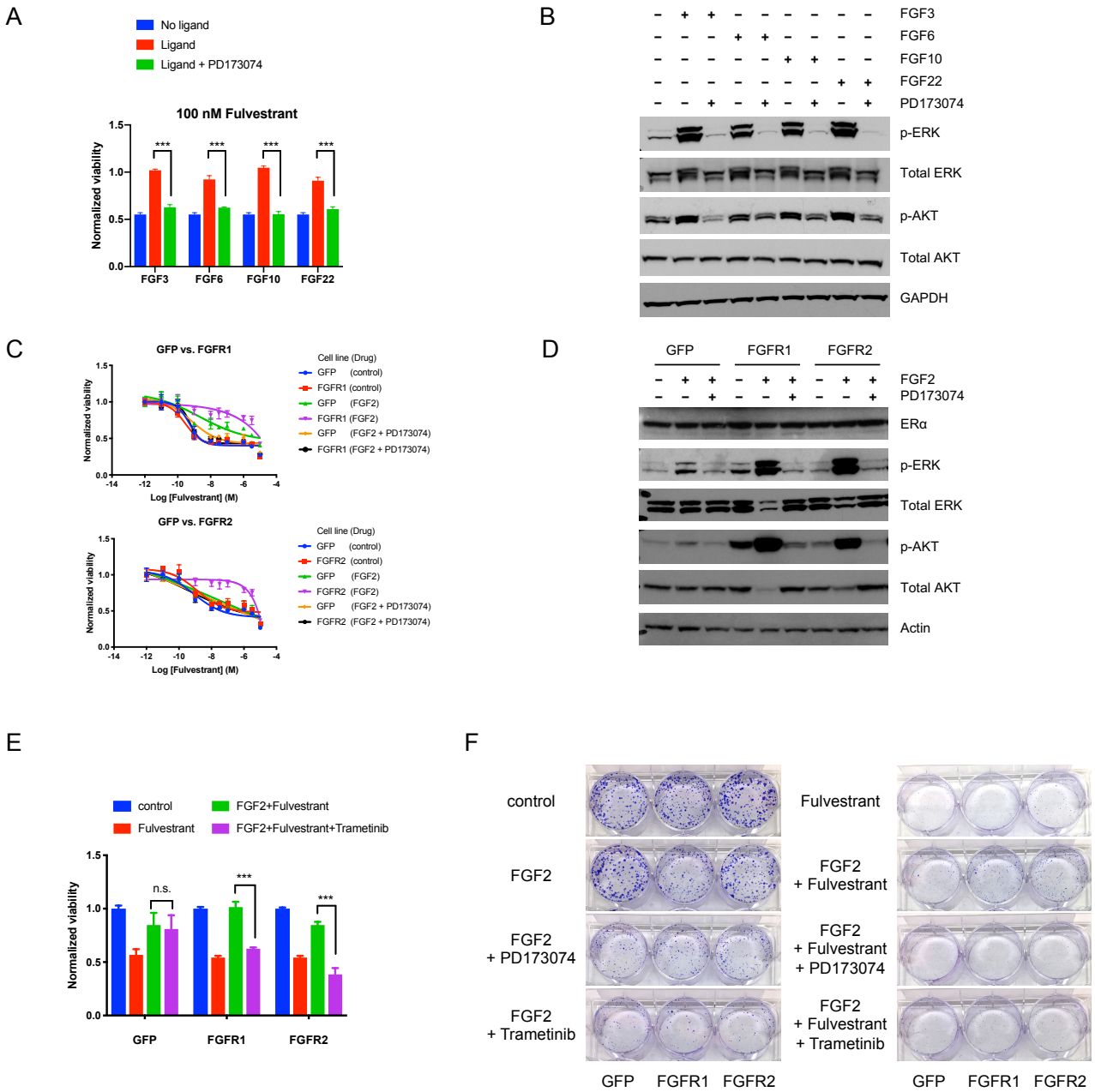

Figure 4. Active FGFR signaling leads to resistance to SERDs through activation of MAPK pathway. A, FGF ligands lead to resistance to fulvestrant, which was blocked by FGFR inhibitor PD173074. Recombinant FGF ligands were added into media every three days at the concentration of 100 ng/mL with or without 1 μM PD173014. T47D cells were treated with heparin (1 μg/mL) that facilitates the binding between FGF ligand and receptor, and sensitivity to 100 nM fulvestrant over six days was normalized to DMSO control. *** p-value < 0.001. Student t-test was performed for pair-wise comparisons. Results shown are ± SD and representative of three independent experiments. B, FGF ligands increased ERK and AKT phosphorylation, which was blocked by PD173074. T47D cells were treated as indicated for one hour before protein harvest for western blot. Results shown are representative of two independent experiments. C, FGFR1 or FGFR2 overexpression leads to resistance to fulvestrant, which was blocked by PD173074. GFP, FGFR1 or FGFR2 was overexpressed in T47D cells to establish stable T47D_GFP, T47D_FGFR1 and T47D_FGFR2 cells. The fulvestrant sensitivity of various cell lines were determined in the presence or absence of 10 ng/mL FGF2 and 1 μM PD173074 over six days of drug treatment. Results shown are ± SD and representative of three independent experiments. D, FGFR1 and FGFR2 induced phosphorylation of ERK and AKT in the presence of FGF2, which was blocked by PD173074. Results shown are representative of two independent experiments. Cells were treated with indicated conditions for one hour before protein harvest. E and F, Trametinib abrogated the resistance to fulvestrant conferred by FGFR1 or FGFR2. Cells were treated with different conditions as indicated: 10 ng/mL FGF2; 100 nM fulvestrant; 500 nM trametinib. CellTiter-Glo assay was performed to measure cell viability after six days for all dose response curves (E), data are ± SD. 2,000 cells were plated on Day 1 and treated on Day 2, and colony formation assay was performed after three weeks of drug treatment (F). Results shown are representative of three and two independent experiments, respectively. * p-value < 0.05, ** p-value < 0.01, *** p-value < 0.001, n.s. not significant. Student t-test was performed for pair-wise comparisons.

Figure 5

A

GFP — Fulvestrant

control	0	0.1 nM	10 nM	1 μM	10 μM
0	1.00	0.93	0.59	0.49	0.32
0.1 nM	1.19	1.06	0.59	0.51	0.30
10 nM	1.14	1.00	0.63	0.56	0.32
100 nM	0.76	0.75	0.47	0.47	0.29
1 μM	0.54	0.47	0.35	0.36	0.24
10 μM	0.25	0.20	0.13	0.20	0.16

+FGF2	0	0.1 nM	10 nM	1 μM	10 μM
0	1.00	0.90	0.63	0.63	0.35
0.1 nM	1.11	1.03	0.71	0.59	0.35
10 nM	1.02	0.99	0.65	0.56	0.30
100 nM	0.75	0.63	0.43	0.41	0.23
1 μM	0.48	0.48	0.34	0.31	0.21
10 μM	0.22	0.26	0.22	0.20	0.14

+FGF2 +FGFRi	0	0.1 nM	10 nM	1 μM	10 μM
0	1.00	0.93	0.66	0.58	0.38
0.1 nM	1.14	1.02	0.72	0.63	0.40
10 nM	1.03	0.97	0.57	0.48	0.30
100 nM	0.86	0.78	0.45	0.39	0.27
1 μM	0.59	0.56	0.41	0.37	0.23
10 μM	0.30	0.30	0.14	0.19	0.15

FGFR1 — Fulvestrant

control	0	0.1 nM	10 nM	1 μM	10 μM
0	1.00	0.91	0.48	0.45	0.25
0.1 nM	1.02	0.92	0.54	0.52	0.28
10 nM	0.92	0.87	0.54	0.51	0.27
100 nM	0.75	0.66	0.37	0.36	0.22
1 μM	0.50	0.47	0.30	0.29	0.19
10 μM	0.26	0.26	0.18	0.17	0.13

+FGF2	0	0.1 nM	10 nM	1 μM	10 μM
0	1.00	1.04	0.90	0.87	0.42
0.1 nM	1.13	1.09	1.03	0.92	0.46
10 nM	1.18	1.26	1.03	1.01	0.51
100 nM	1.08	1.09	0.93	0.86	0.41
1 μM	0.76	0.75	0.70	0.69	0.32
10 μM	0.33	0.37	0.29	0.30	0.09

+FGF2 +FGFRi	0	0.1 nM	10 nM	1 μM	10 μM
0	1.00	0.90	0.53	0.52	0.26
0.1 nM	1.01	0.90	0.56	0.51	0.28
10 nM	0.98	0.77	0.52	0.46	0.24
100 nM	0.70	0.67	0.38	0.38	0.23
1 μM	0.53	0.46	0.33	0.29	0.18
10 μM	0.14	0.14	0.11	0.11	0.08

FGFR2 — Fulvestrant

control	0	0.1 nM	10 nM	1 μM	10 μM
0	1.00	0.98	0.59	0.55	0.35
0.1 nM	1.09	1.08	0.62	0.59	0.37
10 nM	1.06	1.00	0.56	0.53	0.34
100 nM	0.72	0.68	0.44	0.40	0.30
1 μM	0.55	0.59	0.37	0.38	0.28
10 μM	0.25	0.28	0.19	0.20	0.18

+FGF2	0	0.1 nM	10 nM	1 μM	10 μM
0	1.00	1.00	0.84	0.87	0.56
0.1 nM	1.15	1.13	1.00	0.94	0.58
10 nM	1.10	1.13	0.97	0.96	0.53
100 nM	1.06	0.84	0.90	0.84	0.49
1 μM	0.79	0.78	0.63	0.60	0.35
10 μM	0.31	0.35	0.29	0.31	0.15

+FGF2 +FGFRi	0	0.1 nM	10 nM	1 μM	10 μM
0	1.00	0.94	0.51	0.53	0.32
0.1 nM	0.95	0.92	0.54	0.52	0.33
10 nM	0.90	0.87	0.49	0.48	0.31
100 nM	0.63	0.61	0.39	0.40	0.26
1 μM	0.54	0.53	0.39	0.37	0.27
10 μM	0.25	0.24	0.19	0.20	0.16

B

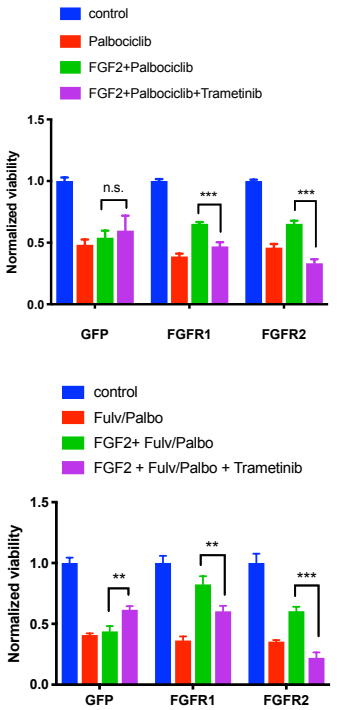

C

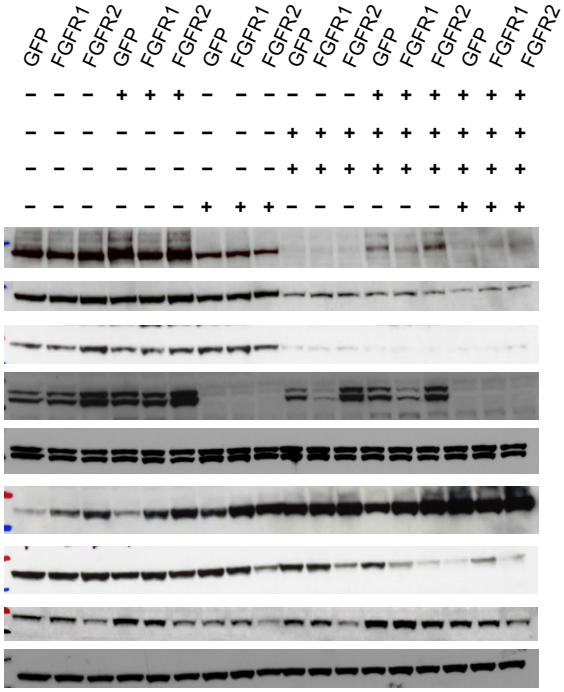

Figure 5. **Active FGFR signaling leads to resistance to the combination of SERDs and CDK4/6 inhibitors.** A, T47D_GFP, T47D_FGFR1 and T47D_FGFR2 cells were treated with the combination of fulvestrant and palbociclib at various doses for six days. The percentage of cell survival shown was normalized to DMSO control for each condition. The combination treatment was carried out under three conditions: 1, control; 2, with 10 ng/mL FGF2; 3, with 10 ng/mL FGF2 and 1 μM PD173074 (FGFRi), with media refreshed every three days. Results shown are representative of three independent experiments. B, MEK inhibitor trametinib abrogated the resistance to palbociclib alone (Top panel) or the combination of fulvestrant and palbociclib (Bottom panel) conferred by FGFR1 or FGFR2. Cells were treated with different conditions as indicated for six days before CellTiter-Glo assay. Concentration of drugs used: 10 ng/mL FGF2; 100 nM fulvestrant (Fulv); 1 μM palbociclib (Palbo); 500 nM trametinib. * p-value < 0.05, ** p-value < 0.01, *** p-value < 0.001. n.s. not significant. Student t-test was performed for pair-wise comparisons. Results shown are ± SD and representative of three independent experiments. C, Trametinib blocked ERK phosphorylation and reduced CCND1 and p-Rb levels. Cells were treated as indicated daily for two days before protein harvest and western blot. Results shown are representative of two independent experiments.

Figure 6

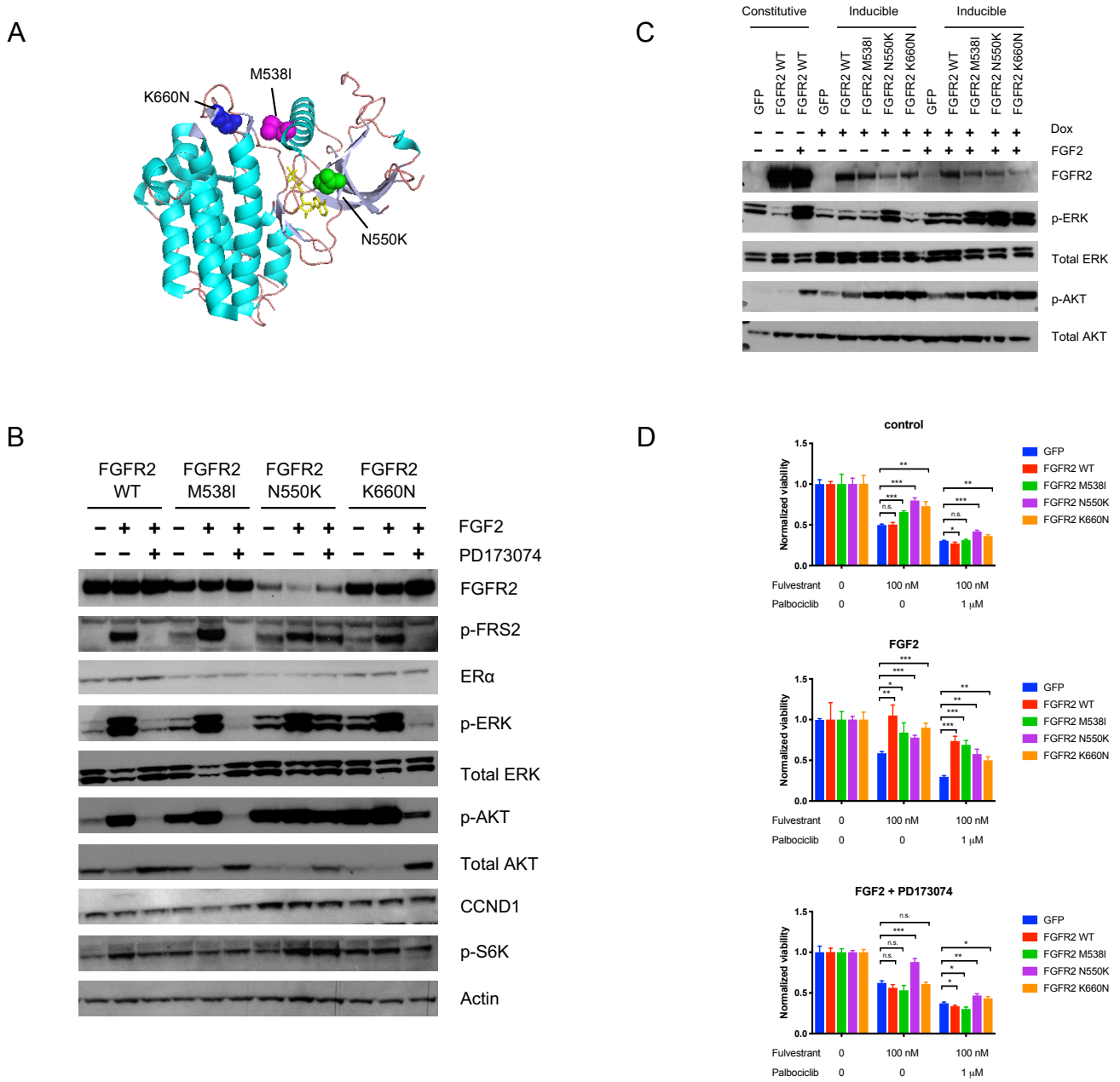

Figure 6. FGFR2 M538I, N5550K and K660N were activating mutations and conferred resistance to fulvestrant and/or palbociclib. A, Crystal structure of activated FGFR2 protein with mutations shown. FGFR2 is in complex with ATP analog (in yellow) and substrate peptide (PDB ID: 2PVF). B, Stable cell lines overexpressing FGFR2 wildtype (WT), M538I, N550K, and K660N were treated with 10 ng/mL FGF2 and/or 1 μM PD173014 for one hour before protein harvest. Results shown are representative of two independent experiments. C, Tetracycline-inducible cell lines that express FGFR2 WT, M538I, N550K and K660N were established and treated with 100 ng/mL doxycycline (Dox) to induce gene expression. Before protein harvest, cells were treated with doxycycline 24 hours before FGF2 stimulation for 3 hours followed by another 3 hours of FGF2 stimulation. Cells were treated with heparin (1 μg/mL) that facilitates the binding between FGF2 and FGFR2. Protein lysates from T47D cells expressing GFP and T47D cells with constitutive overexpression of FGFR2 were used as control. Results shown are representative of three independent experiments. D, Stable cell lines constitutively overexpressing GFP or FGFR2 constructs (as previously described) were examined for sensitivity to fulvestrant or combination of fulvestrant and palbociclib with or without the treatment of FGF2 and/or PD173074. * p-value < 0. 05, ** p-value < 0.01, *** p-value < 0.001, calculated as compared to GFP group in all conditions. Student t-test was performed for pair-wise comparisons. Results shown are ± SD and representative of three independent experiments.

Figure 7

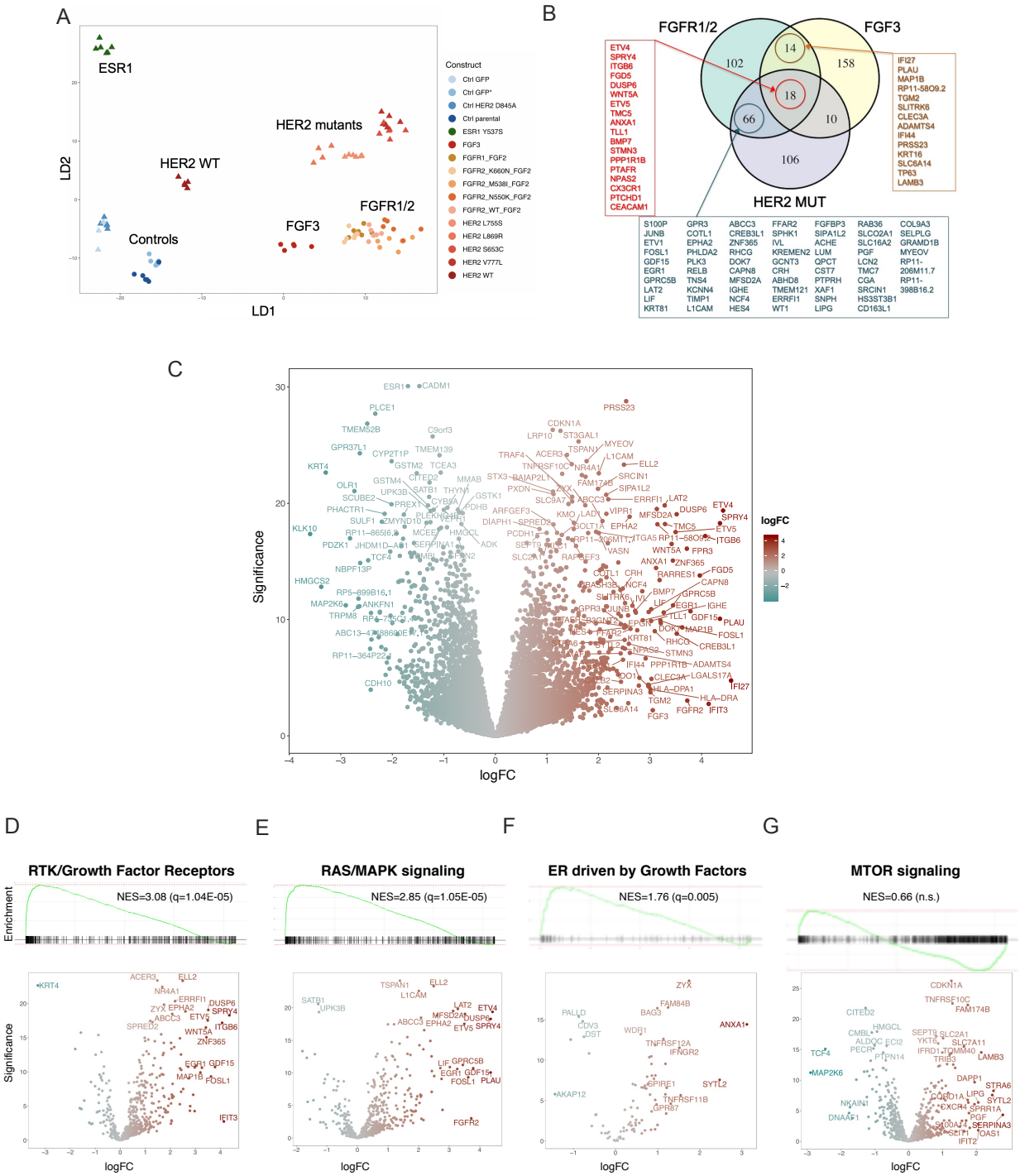

Figure 7. Transcriptional cell-state analysis of FGF/R activating perturbations reveals a distinct cell-state associated with MAPK activation and ER-reprograming. A, Linear Discriminant Analysis (LDA) projection of FGFR/FGF-activated cells and controls. Two-dimensional visualization of in the transcriptional footprints driven by FGF3, FGFR1, FGFR2, FGFR2 activating mutants, and GFP, as well as HER2 activating mutants, wild-type HER2, kinase-dead HER2 D845A, and ESR1 Y537S (previously published, with data points from HER2 study indicated by triangles [11]), all treated with DMSO. B, Venn diagram showing commonalities and differences among upregulated genes for cells expressing FGFR (FGFR1, FGFR2, and FGFR2 activating mutants), FGF3, and HER2 activating mutants. Upregulated genes are based on log fold change (logFC) comparing the activating constructs and controls under DMSO. C, Gene Set Enrichment Analysis (GSEA) plots and Volcano plot representation of differentially expressed genes (DEGs) comparing the transcriptional footprints from cells expressing FGFR1, FGFR2, FGFR2 activating mutants, and FGF3, collectively vs. controls, all under DMSO. The FGF/R-ACT transcriptional state was derived from significant DEGs. D-G, Selective volcano plots and GSEA plots indicate several pathways which are activated in the FGF/R-ACT state: D, RTK/Growth Factor Receptors signaling genes (624 genes), E, RAS/MAPK genes (701 genes). F, ER signaling driven by Growth Factors genes (95 genes), G, MTOR pathway genes (953 genes). See Supplemental Table.11 for gene sets, Supplemental Table.12 for a comprehensive list of gene sets and pathway associations. NES, normalized enrichment score; n.s. not significant.

Figure 8

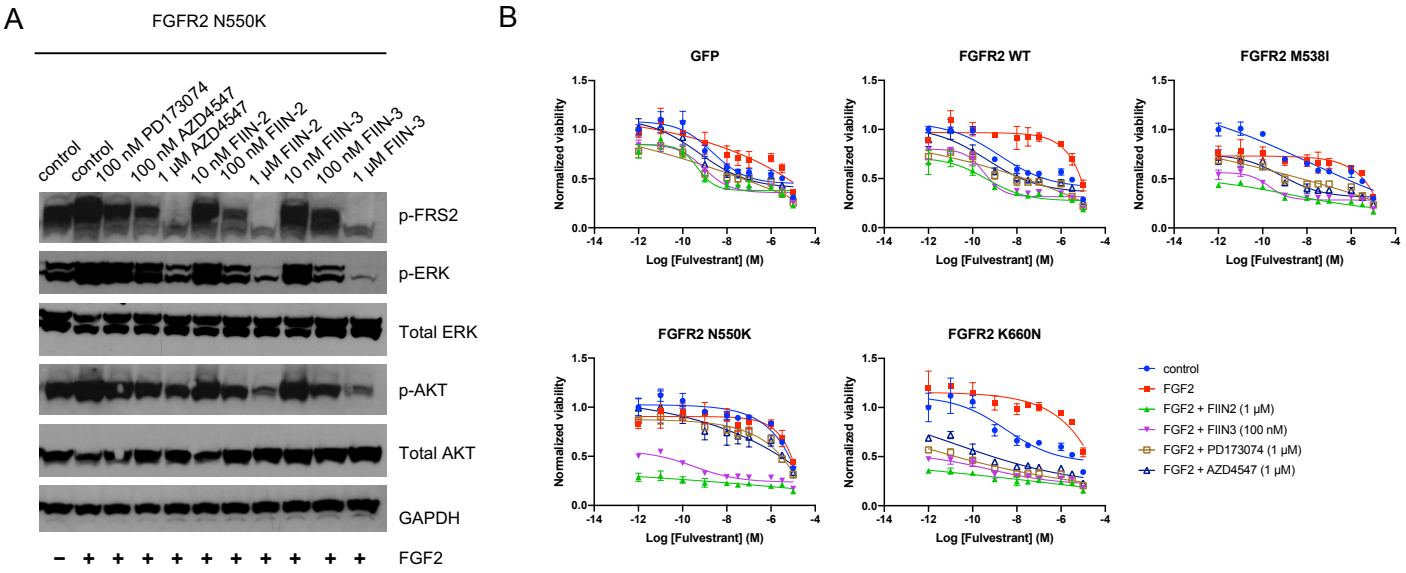

Figure 8. Activating FGFR2 mutations were targeted by irreversible kinase inhibitors FIIN-2 and FIIN-3. A, T47D cells overexpressing FGFR2 N550K cells were treated as indicated for three days and retreated for three hours before protein harvest and western blot. Results shown are representative of two independent experiments. B, All stable cells lines expressing GFP or FGFR2 constructs were treated with fulvestrant under the following conditions: control, 10 ng/mL FGF2, 10 ng/mL FGF2 with 1 μM AZD4547, 10 ng/mL FGF2 with 1 μM FIIN-2, or 10 ng/mL FGF2 with 100 nM FIIN-3. Drug response curves were determined by CellTiter-Glo. Results shown are ± SD and representative of three independent experiments.

Figure 9

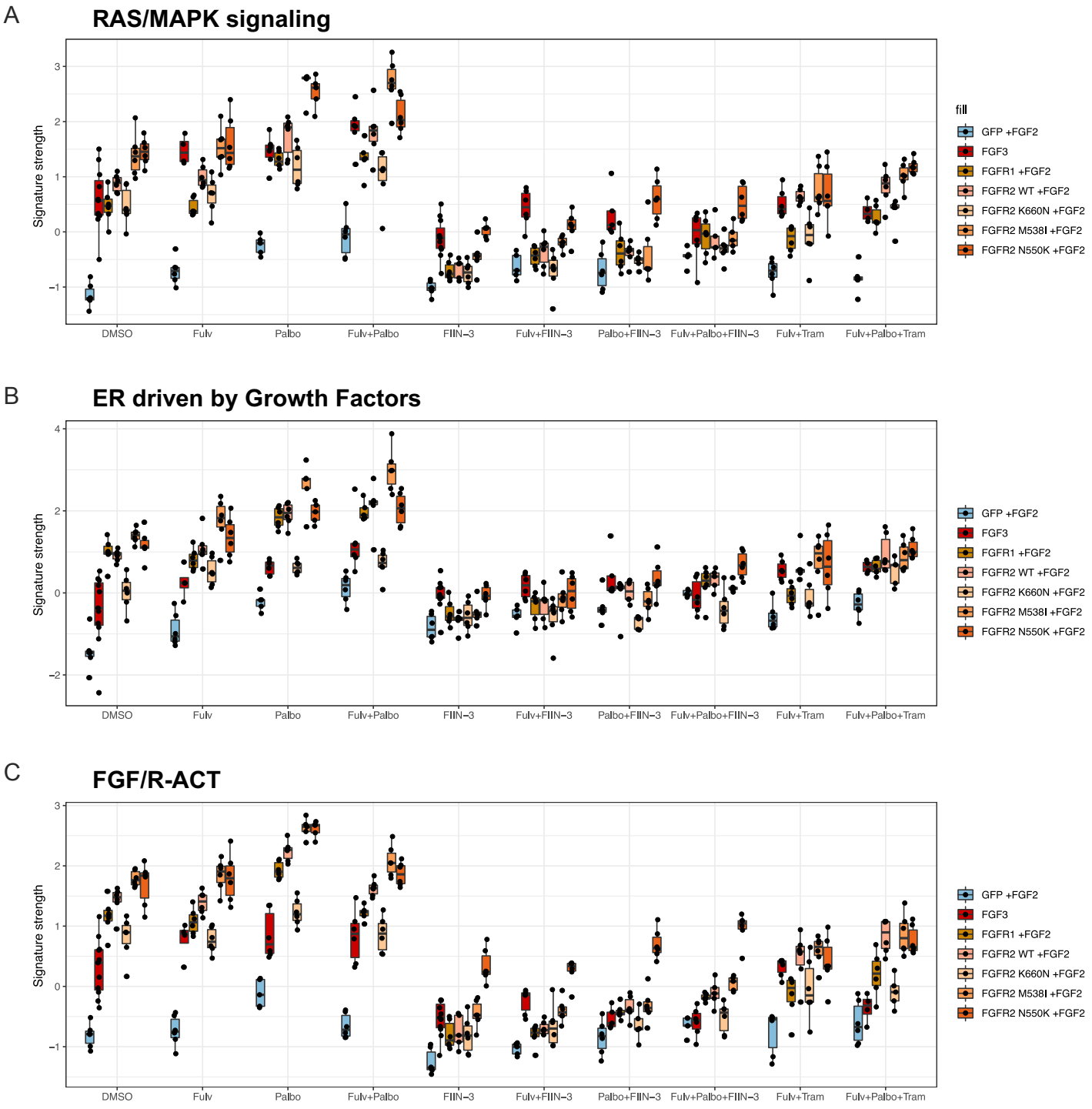

Figure 9. RNA-seq measurement of oncogenic signatures reflects differential sensitivity of FGF/R activating perturbations under various drugs. Three oncogenic signatures were compared across various drug conditions for resistant FGFR/FGF cell lines. A, RAS/MAPK signature. B, ER signaling driven by growth factors signature. C, FGF/R-ACT signature. The signature strength for each sample is depicted in the Y-axis with a Z-score scaled across all 647 samples. Each box plot represents the distribution of the signature strength among replicates of each experimental condition as indicated. Drug conditions include: "DMSO" (No Drug), "Fulv" (Fulvestrant), "Palbo" (Palbociclib), "Fulv+Palbo" (Fulvestrant and Palbociclib), "FIIN-3", "Fulv+FIIN-3" (Fulvestrant and FIIN-3), "Palbo+FIIN-3" (Palbociclib and FIIN-3), "Fulv+Palbo+FIIN-3" (Fulvestrant, Palbociclib and FIIN-3), "Fulv+Tram" (Fulvestrant and Trametinib), "Fulv+Palbo+Tram" (Fulvestrant, Palbociclib and Trametinib. Construct perturbations include overexpression of GFP (Control), FGF3, FGFR1, and FGFR2 (WT, K660N, M538I and N550K). For cell lines overexpressing FGFR1/2, FGF2 was supplemented in the media. See Supplementary methods for details and Supplemental Table.11 for gene sets definitions.

Figure 10

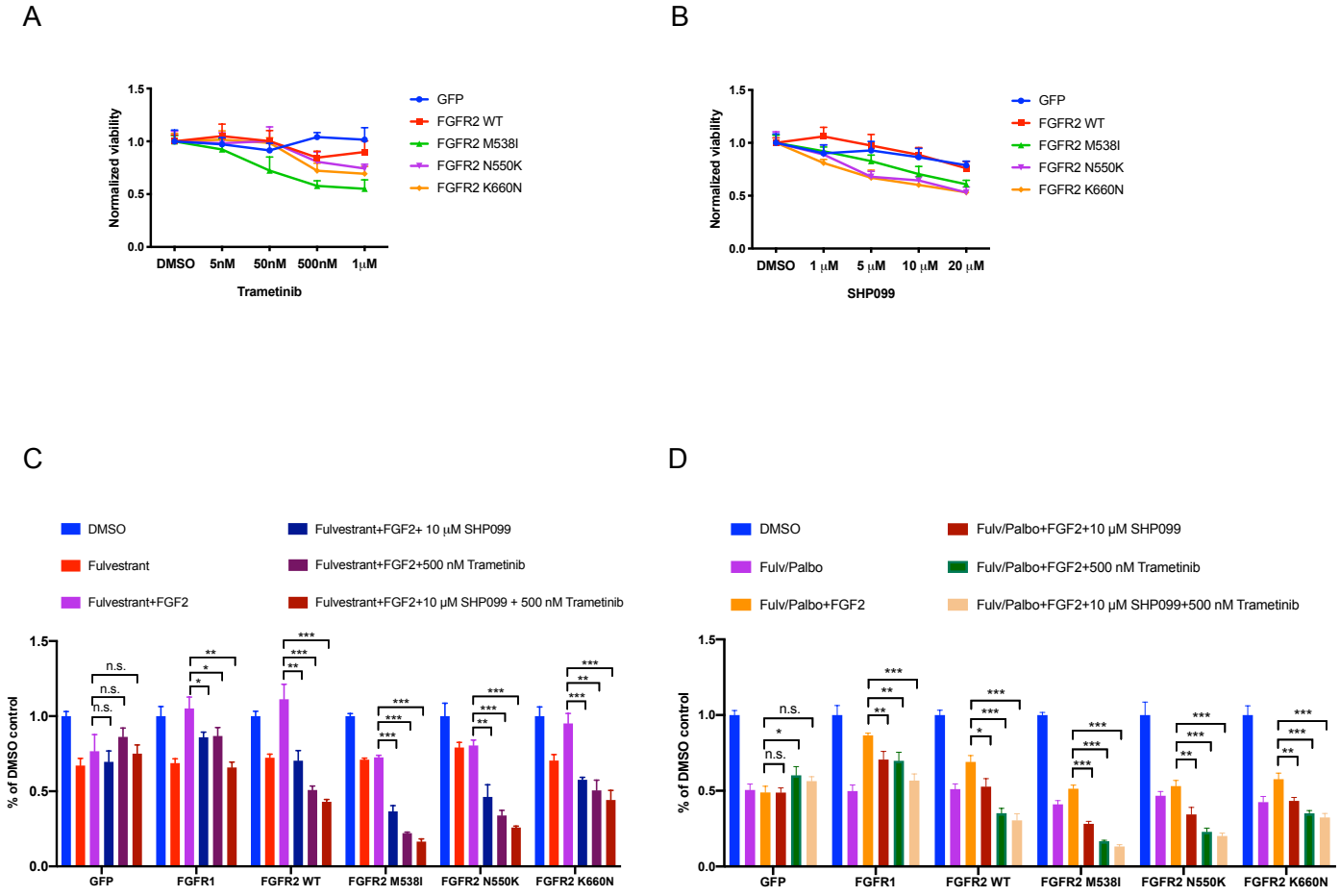

Figure 10. FGFR-induced resistance phenotype was reversed by MEK and SHP2 inhibition. A and B, Trametinib (A) and SHP099 (B) sensitivity of T47D cell lines expressing GFP or different FGFR2 constructs was examined respectively. Results shown are ± SD and representative of two independent experiments. C and D, SHP099 as a single agent and in combination with trametinib rescued resistance to fulvestrant (C) and/or palbociclib (D) conferred by FGFR1 or FGFR2 wildtype and mutant constructs. Concentration of drugs used: 10 ng/mL FGF2; 100 nM fulvestrant; 1 μM palbociclib; 500 nM trametinib; 10 μM SHP099. * p-value < 0.05, ** p-value < 0.01, *** p-value < 0.001. n.s. not significant. Student t-test was performed for pair-wise comparisons. Results shown are ± SD and representative of three independent experiments.